ROLE OF DUST GRAINS ON FAST WAVE STABLIZATION/DESTABLIZATION OF DRIFT WAVE IN PLASMA

Thesis Submitted in partial fulfillment of the requirements for the degree

Of

MASTER OF TECHNOLOGY

In

NUCLEAR SCIENCE & ENGINEERING (NSE)

Submitted by

MRITYUNJAY KUMAR SINGH

(2K13/NSE/10)

Under the Supervision of

Prof. SURESH C. SHARMA

Head, Department of Applied physics

Delhi Technological University

Delhi, India

DEPARTMENT OF APPLIED PHYSICS
DELHI TECHNOLOGICAL UNIVERSITY,
SHAHBAD, DAULATPUR, DELHI - 110042

JULY-2015

DELHI TECHNOLOGICAL UNIVERSITY

Established by Govt. of Delhi vide Act 6 of 2009

(Formerly Delhi College of Engineering)

SHAHBAD DAULATUR, BAWANA ROAD, DELHI-110042

CERTIFICATE

This is to certify that work which is being presented in the dissertation entitled **ROLE OF DUST GRAINS ON FAST WAVE STABILIZATION/DESTABILIZATION OF DRIFT WAVE IN PLASMA** is the authentic work of **MRITYUNJAY KUMAR SINGH** under my guidance and supervision in the partial fulfillment of requirement towards the degree of **Master of Technology in Nuclear Science & Engineering** run by Department of Applied Physics in Delhi Technological University during the year 2013-2015.

As per the candidate declaration this work has not been submitted elsewhere for the award of any other degree.

Prof. SURESH C. SHARMA
Head, Department of Applied Physics
Delhi Technological University

Delhi-110042

Department of Applied Physics

Delhi Technological University

DECLARATION

We hereby declare that the project entitled "**ROLE OF DUST GRAINS ON FAST WAVE STABLIZATION/DESTABLIZATION OF DRIFT WAVE IN PLASMA**" submitted by us in the partial fulfillment of the requirements for the award of the degree of Master of Technology (Nuclear science and Engineering) of Delhi Technological University (DTU), is record of our own work carried under the supervision and guidance of **Prof. SURESH C. SHARMA** (Head, Department of Applied Physics).

To the best of my knowledge this project has not been submitted to Delhi Technological University (DTU) or any other University or Institute for the award of any degree/Diploma.

MRITYUNJAY KUMAR SINGH

(2K13/NSE/10)

ACKNOWLEDGEMENT

I am extremely thankful to my mentor, **Prof. SURESH C. SHARMA**, professor and HOD, Department of Applied Physics, Delhi Technological University, Delhi for his exemplary guidance, monitoring and constant encouragement throughout the M. Tech course. I would also like to thank our friends and teacher for their cooperation and suggestion during the preparation of this project report.

.

MRITYUNJAY KUMAR SINGH
(Roll. No. 2K13/NSE/10)
M.Tech (Nuclear Science & Engineering)
Department of Applied Physics
Delhi Technological University

ABSTRACT

We have examined the role of dust grains on fast wave stabilization/destabilization of drift wave in plasma. We have found the growth rate of the mode increases with the relative density of dust grain. We have also found that the value of growth increases with decreasing the dust grain size and dust grain density.

TABLE OF CONTENTS

LIST OF FIGURES

LIST OF SYMBOLS

$-e$	Electronic charge
m_{0e}	Mass of electron
m_{0i}	Mass of ion
m_{0D}	Mass of dust
a	Dust grain size
T_e	Temperature of electron
T_i	Temperature of ion
ϕ	Electrostatic potential
ϕ_m	Pondermotive potential
F_p	Pondermotive force
$B_0\hat{z}$	Static magnetic field
ω_{ce}	Electron cyclotron frequency
ω_{ci}	Ion cyclotron frequency
ω_p	Plasma frequency
ω_{cD}	Dust gyro-frequency
ω_{pD}	Dust charge frequency
L_n	Density scale length
$\vec{v}_{ed}$	Electron drift velocity
$\vec{v}_{id}$	Ion drift velocity
v_{the}	Electron thermal velocity
v_{thi}	Ion thermal velocity
$\vec{J}^{NL}$	Non linear current density
ε_0	Free space permittivity

n_{1e}	Electron density perturbation
n_{1i}	Ion density perturbation
n_{1D}	Dust density perturbation
Q_{0D}	Charge of dust
χ_{1e}	Electron susceptibility
χ_{1i}	Ion susceptibility
χ_d	Dust susceptibility
λ_{eD}	Electron Debye length
c_s	Speed of sound
β	Coupling factor
χ'_{1e}	Electron susceptibility with dust
χ'_{1i}	ion susceptibility with dust
η	Charging rate of dust
δ	Relative density of dust grain size
γ	Growth rate

CHAPTER 1

INTRODUCTION

1.1 WHAT IS PLASMA?

"Jan Evangelista Purkinje" a Czech scientist pioneered a Greek word "Plasma" which means “produced” or “generated”[1]. The phase transformation in any substance can be achieved by providing heat energy larger than the binding energy of substance. In Figure 1.1 the transformation among various states of water by increment of temperature is shown, various kind of plasmas and equivalent state of matter occurs in these ranges [2]. Route to the fourth state of matter, which is named plasma, begins from initial state ice (solid) then ice on heating transforms into water (liquid-second state), water then transforms into steam (third state) and then finally into ionized gas (fourth state). In case of plasma thermal energies are higher than binding energies and it is basically an ionized quasi-neutral gas and the interaction between the charged particles is mainly collective as many particles, through their large range electromagnetic fields, interact simultaneously.

Theoretically different types of plasma exist depending upon the variety of species in it. The most common case is the electron-ion plasma and other cases are the electron-positron plasma, electron-hole plasma (semiconductor plasma), electron-positron-ion plasma and the electron-ion-dust plasma. The presence of charge free molecules decide the level of ionization of plasma i.e., if charge free particles are available, it is called incompletely ionized plasma generally completely ionized plasma. In this investigation, it was considered the completely ionized case for electron-particle plasma and the electron-particle dust plasma called as dusty.

The basic plasma parameters are the temperature T, the density n_0 and the magnetic field B_0 generally calculated in electron-Volt (eV), respectively. These three parameters bring forth the three subsidiary parameters i.e., these three parameters bring forth the three auxiliary parameters i.e., the thermal speed (v_{th}), the plasma frequency (ω_p) and cyclotron frequency.

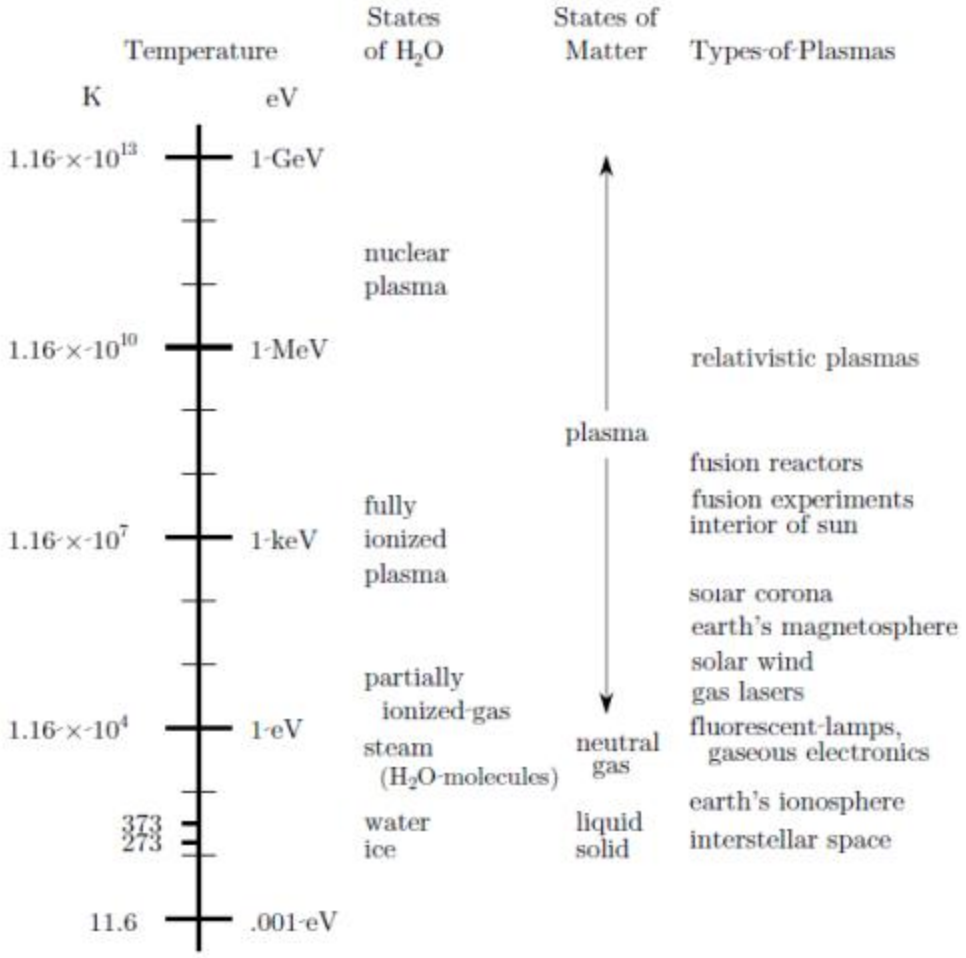

Figure1.1: Schematic of changing in the states of water by increasing the temperature[35].

The proportion of distinctive blends of these subsidiary parameters leads to the well-known derived quantities the Debye length $\lambda_D = (T/4\pi n0e^2)^{1/2}$, Larmor radius $r_L = v_{th}/\omega_c$ and the plasma beta $\beta_\alpha = 8\pi n_0 T_\alpha / B^2_0$. The derived quantities are used to characterize the different plasma environments.

The plasma variables are the wave frequency ω and the wave vector k which focus the time scale and the length size of a phenomenon under observation. The wave frequency (ω), wave vector (k) articulates the time scale (length scale) is fast or slow (long or short) as compared to the characteristic frequency (length) of the particles i.e., plasma frequency or the cyclotron frequency (Debye length or Larmor radius). The ratio of the wave frequency to the wave vector ($\omega /k = v_\varphi$) defines phase speed of the wave and can be compared with the thermal speed v_{th} of particular species to analyze the dispersion characteristics of the wave.

1.2 PRODUCTION OF PLASMAS

By raising the temperature of substance till a reasonably high fractional-ionization is produced, plasmas can be obtained. The electron temperature and the degree of ionization are closely related under thermodynamic equilibrium conditions. By ionization process we can obtain plasma. Plasma raises ionization degree higher than its thermal equilibrium value. Ionization occurs by absorbing incident photons in the case of photo ionization process, in which energy is equivalent to or higher than the ionizing potential of the absorbing atoms. The surplus-energy of photons are transformed 910 A^0.

The recombination usually occurs so fast in the laboratory leading to complete disappearance of the plasma within a small fraction of a second [4].

1.3 WHAT IS USED OF PLASMA?

Most practical and important application plasma lies in future. The major method in practice for generating electric power is to use sources of heat to get steam from water, which drives turbo generators. Sources of heat depend on the combustion of oil, coal, and natural gas (all fossil fuels), and on the fission process in a very high amount of heat-energy of H-atom, He-atom & the neutrons. By absorption of these particle loss & also inefficient heat to electricity conversion. At a particle density in volume 10^{20} m^{-3}, for e.g., the containment-time must be 1s. Although there are much progress but still such figures are yet to be achieved. Fusion reactor may also desalinate seawater in addition to generating power. Around 66.67% of the land surface in the world is uninhabited, of which 50% of the area is arid. The use of both giant fusion and fission reactors in evaporating the seawater on large scale can make irrigating such arid areas economically viable. The elimination of the heat-steam-mechanical energy chain is another possibility in power-production [1].

For accelerating plasma, thermo effect which is the inverse of the dynamo into plasmas, it is possible achieving thrust that is directly-proportional to the square of magnetic-field. For the propulsion of spacecraft in deep-space motors, based on such techniques have been proposed. The advantage of using such motors is that they can achieve very high exhaust-velocities, thus it will minimize fuel consumption [2].

1.4 DUST IN PLASMA

Dust is omnipresent in plasmas [2]. Its cause fluctuates with environment. For instance, in space it might be delivered as an aftereffect of an impact between space rocks, though in a Tokamak it might be created by vast disturbances. Dust is made out of a scope of components relying upon the earth, mostly water in Saturn's rings, though it might be hydrocarbons and tungsten mixes in Tokamaks. As dust in plasma is normally charged, its vicinity in vast amounts will fundamentally modify the plasma parameters by limiting a lot of charge in the dust grain volume. The connection between charged grains includes an additional level of multifaceted nature, which urges a few creators to coin the term 'complex plasma' for the three part clean particle electron plasma. I feel this is to some degree liberal, as two segment plasmas are likewise rather tricky. I will consequently allude to 'dusty plasmas'.

1.5 NON-FUSION DUSTY PLASMAS

This investigation is fundamentally concerned with fusion plasmas, particularly Tokamaks, and hence won't focus on the substantial measure of work led on dusty plasma crystals and space plasmas. In any case, these other principle zones of dusty plasma interest will be outlined in the accompanying areas.

1.6 DUST IN ATMOSPHERIC AND SPACE PLASMAS

Space plasmas change enormously, stars are greatly hot thick objects, though the interstellar medium has a temperature of just 3 K. There are in this way numerous intriguing situations where dust exists in expansive amounts: planetary rings, planetary cloud, and interstellar space and comet radiances to give some examples. The interstellar medium is brimming with dust, either remainders of crashes between expansive articles, comet trash or scraps from stellar and planetary arrangement. The particles are generally exceptionally diffuse and made for the most part out of carbon. NASA routinely gathers tests in the Earth's stratosphere, and they are rocks 5-20 mm in distance across [2]. Planetary rings present diverse dust situations. All the substantial gas goliaths have ring frameworks, delivered either from satellites tore

separated by tidal powers, or meteor sways. Saturn has the most celebrated ring framework (Figure 1.2), on the grounds that the principle rings are generally obvious with a telescope.

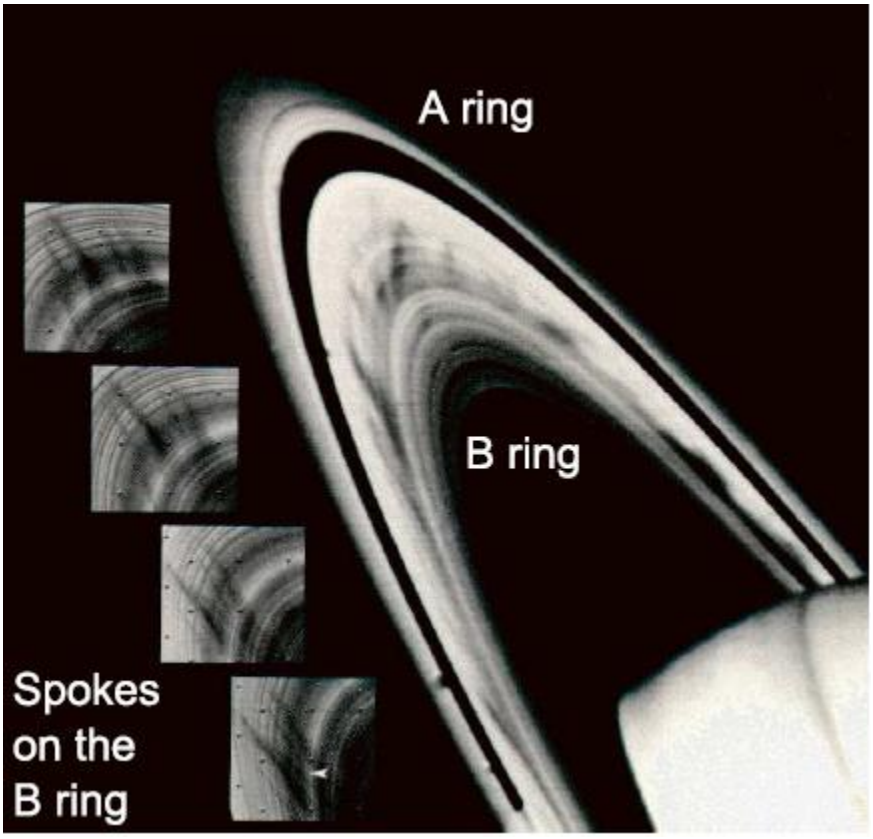

Figure 1.2: Saturn's rings; the dark features are "spokes".[38]

The particles are made for the most part out of ice, yet shift from microns to meters in size. The biggest dust grains exist in Saturn's fundamental rings, the A and B ring. All in all, they are uncharged since there is no plasma around them. The sheer measure of material in the A and B rings retains any ionized particles delivered by photoionisation. The high electron versatility along attractive field lines opposite to the ring plane implies that any electrons that escape from the ring plane skip once more from the posts and are retained. In any case, there is confirmation of some charged dust particles suspending far from the B ring, from dull components called spokes which are seen to be moving with planet's attractive field. These are ineffectively caught on. Bunches of little (nm estimated) charged particles may exist in the weak E ring (not unmistakable in figure 1.2), where there is a lower centralization of material. Comets are articles made of different dust materials, predominantly carbon, blended with solidified gasses. They are

thought to exist in an extensive cloud far outside the nearby planetary group, the Oort cloud. Those that enter the close planetary system dissipate as they close to the sun, framing a state of insensibility of diffuse material. They add to two tails, a particle tail and a dust tail. Dust grains in the trance like state fluctuate from hundredths of microns to microns in size. The Earth's upper environment is a plasma. Specifically noteworthy to dusty plasma specialists is the mesosphere, where one watches noctiluscent mists (NLCs). These structures in the polar mesopause, the highest point of the mesosphere where the temperature is most minimal, especially amid the late spring. An eccentricity of the polar mesopause is that it is colder in the late spring than in the winter [2]. NLCs are made out of sub-micron size ice crystals and sparkle splendidly enough to be seen around evening time. Enthusiasm for these has expanded subsequent to the revelation of polar mesosphere summer echoes (PMSEs), out of the blue solid radar echoes from the mesopause. Some hypothetical work has been directed on a conceivable system for PMSEs including charged dust. The dust is seen as a noteworthy charge transporter, and the charge thickness of the dust can shift essentially over a couple meters [3]. This solid impact of dust on the plasma conditions may adjust the wave-plasma communication enough to clarify the radar reverberation.

CHAPTER 2

DRIFT WAVE AND TOKAMAK

2.1 DRIFTS IN PLASMAS

Quite accurate analytical solution of the drift-velocity of charged-particles may be determined in arbitrary complex electric & magnetic-fields which are slow and steadily varying in both space & time. Solving the Lorentz equation solutions of drift velocity can be obtained [6].

$$m\frac{\partial v}{\partial t} = q\left(\vec{E} + v \times \vec{B}\right) \tag{2.1}$$

The value of this steady-drift is easily measured by assuming the presence of a constant perpendicular drift-velocity in the Lorentz-equation, and then averaging out the cyclotron motion

$$\vec{E} + \langle v \rangle \times \vec{B} = 0 \tag{2.2}$$

Taking cross-product with B in above eq. we obtain

$$V_E = \langle v \rangle = \frac{\vec{E} \times \vec{B}}{B^2} \tag{2.3}$$

This we call 'E-cross-B' drift. General force-drift-velocity can easily be obtained from E×B drift by simply replacing E → F/q in the Lorentz equation as-

$$V_F = \frac{\vec{F} \times \vec{B}}{B^2 q} \tag{2.4}$$

Comparing above equations lead to two very important inferences. First is that a bulk motion, with the V_E velocity, of the whole plasma across magnetic-field takes place due to electric-field which is perpendicular to magnetic-field but do not drive currents into plasma. On the other hand, a cross field-current is driven by the force perpendicular to the magnetic-field due to charged particle's (electrons & ions) motion in the opposite directions.

2.2 NON-UNIFORM MAGNETIC-FIELD DRIFT

For uniform magnetic-field, expression for drift-velocity is derived above. In case of in-homogenous magnetic-field, with respect to space or/& time, the orbit-theory is employed. In orbital-theory, the ratio of Larmor-radius to scale-length of homogeneity is considered to be small (assumption) and expanded [6].

2.2.1 GRAD-B DRIFT

In case when the field-lines are straight and the density varies, the gradient in the magnetic-field then leads to variations in the Larmor-radius i.e., when Larmor-radius decrease, magnetic-field increase and vice-versa. The grad-B drift is perpendicular to both B & ∇B and is proportional to the r_L/L and $v_\perp$ [7] ,which is given by:-

$$v_{\nabla B} = \pm \frac{1}{2} v_{\perp} r_L \frac{\vec{B} \times \nabla B}{B^2} \tag{2.5}$$

The coefficient 1/2 is due to average and ± is the sign of charge indicating that the grad-B drift is in direction opposite to electrons & ions and results in a current which is perpendicular to magnetic-field.

2.2.2 CURVATURE-DRIFT

Let us consider a case where magnetic-field lines are curve with fixed radius of curvature R_c & the strength of magnetic-field do not change. The particles experiences, while moving with velocity $v_{\|}^2$ randomly along the magnetic-field, the centrifugal-force as given by [6]:-

$$F_{fc} = \frac{m v_{\|}^2}{R_c} \hat{r} = \frac{m v_{\|}^2}{R_c^2} \vec{R}_c \tag{2.6}$$

& corresponding drift-velocity becomes

$$V_R = \frac{m v_{\|}^2}{q B^2} \frac{\vec{R}_c \times \vec{B}}{R_c^2} \tag{2.7}$$

When the lines of magnetic-field are curve and its magnitude is also changing, like in case of tokomak-plasma, both grad B drift & curvature-drift are added and the total drift of the particles turns out to be

$$V_R = \frac{m}{q} \frac{\vec{R}_c \times \vec{B}}{B^2 R_c^2} \left(v_{\|}^2 + \frac{v_{\perp}^2}{2} \right) \tag{2.8}$$

2.3 DIAMAGNETIC-DRIFT

In case the plasma is not uniform because of gradient either in temperature or density or in both, the drift-velocity may then be rewritten as [7]:-

$$-\nabla P = -(n k_B T) \tag{2.9}$$

$$v_{dia} = \frac{\vec{B} \times \nabla P}{n q B^2}$$

Such drifts is absent in single-particle theory & illustrates the collective plasma behaviour because this drift involves the plasma pressure which is obtained by considering the moment of the distribution. Both the density & temperature gradient result in non-zero average transverse velocity. Because of the diamagnetic-drift, effective drift-current flows in the plasma due to the motion of charged fluids in opposite direction

2.4 MAGNETIC-CONFINEMENT FUSION

In magnetic-confined plasma like tokamak, drift waves are of great concern. Large amount of dust can be generated in tokamak during a shot by power-flux to surface, especially during disruption. This aspect has two significances: efficiency & safety. The first is related to component's erosion which needs regular replacement & conditioning, and it is also related to impurities which are introduced by the dust evaporating near the plasma core. Second aspect is safety which includes retention of tritium in dust (radioactive hazard), also the large surface-area dust cloud can result in explosion. Furthermore, there is every possibility of cracking of water molecules which can produce highly reactive hydrogen-atoms. Inspite of these facts, little work is done on dust-grain evolution and their movements in the plasma [7].

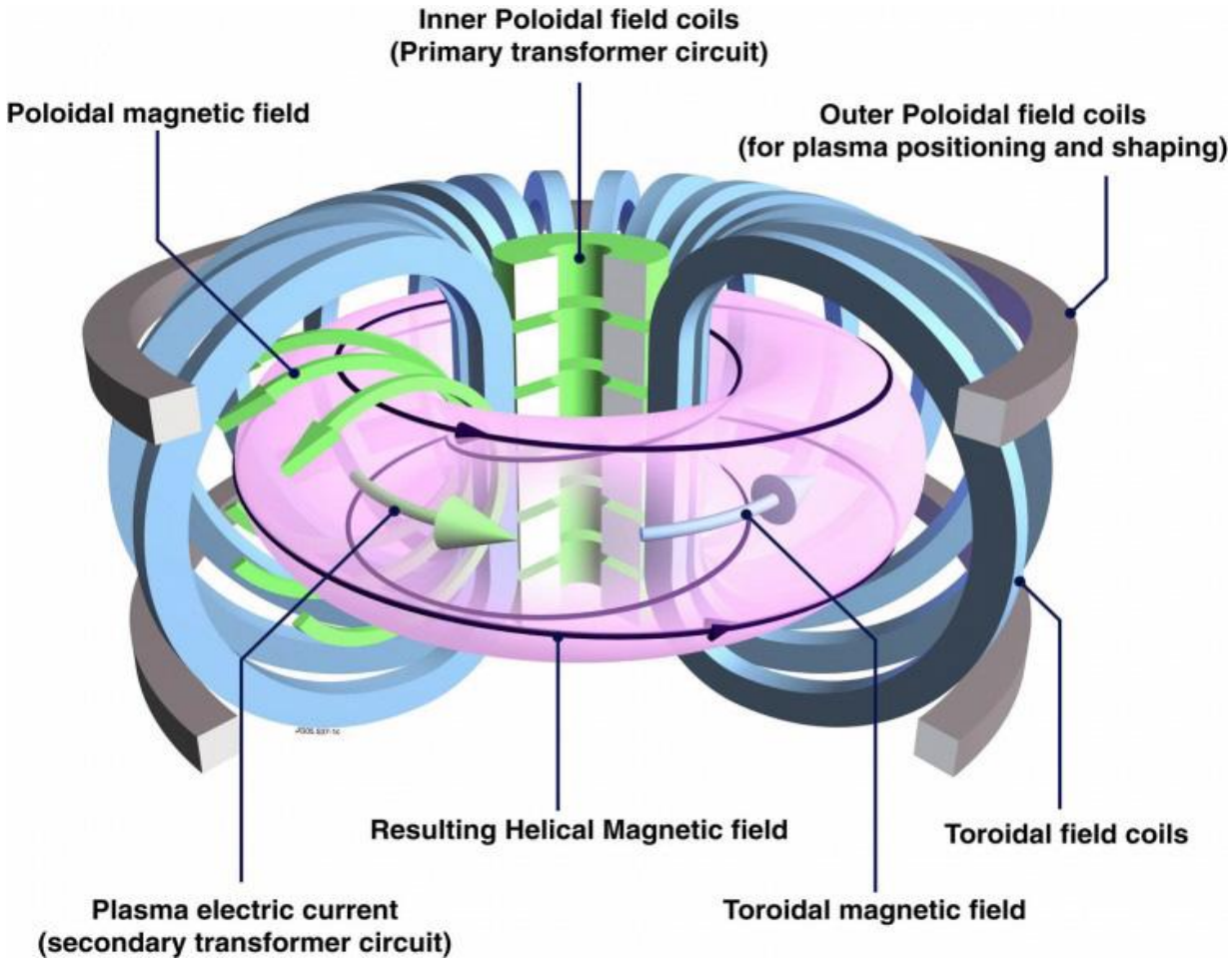

Figure 2-1: Schematic diagram of Tokamak [36]

One way of confining the fuel with such high temperature is to utilize a magnetic-field. At the temperatures important for the fusion reaction, the particles are ionized and the fuel is present in the plasma state. The charged particles begin their helical motion in the plane along the magnetic field. The circular portion of this motion in the plane perpendicular to the field line is called

Gyro-motion [7]. The helical-motion is suitable to keep the plasma, because it doesn't permit the particles to move perpendicular to the magnetic-field; however they are free to move parallel to the magnetic field. The issue of losses at the ends of a linear device can be settled by bending the magnetic-field lines into a torus. Nonetheless, in a toroidal geometry, the magnetic-fields are non-homogeneous. The strength of the magnetic-field is inversely proportional to the distance which is measured from the center of the torus, because of the higher current-density in the toroidal-field coils in the internal side of the torus leads in a stronger magnetic-field. This non-homogeneity prompts to a charge dependent drift (∇B drift), which causes the electrons & ions to drift in vertically opposite directions. The subsequent vertical electric field makes a charge free E×B drift, which moves the whole plasma towards the outside of the torus. This electric field between the top and the base of the torus can be shorted out by helically twisting the magnetic field lines [6].

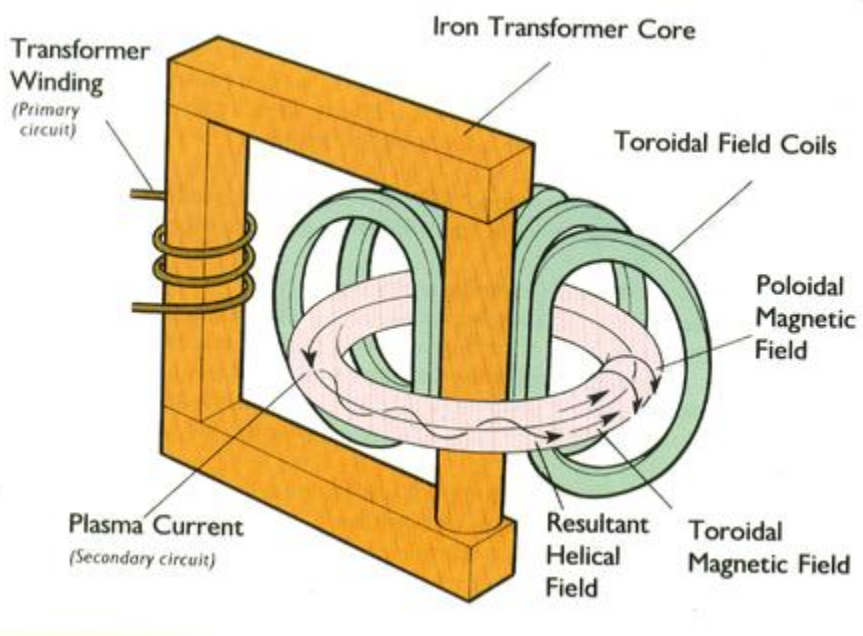

Figure 2-2: Schematic of Tokamak Geometry illustrating poloidal and toroidal direction [40].

A sort of magnetic-confinement device is the tokamak, in which the magnetic-field lines are helically twisted by plasma current. In tokamak geometry, the toroidal direction is the long way whereas the poloidal direction is the short way around the torus. The toroidal plasma current is driven by the transformer coil and it twists the magnetic-field lines as it produces a poloidal -field. The twist of magnetic-field lines is described by the safety-factor. The safety factor ***q*** is the ratio of toroidal transits per single poloidal transit of a magnetic-field line. Because of the

axisymmetry of a tokamak device, the magnetic field lines are composed into magnetic flux surfaces. Along the magnetic field lines, the particles move freely, thus the plasma parameters on the magnetic flux surfaces are adjusted very quickly, while the transport perpendicular to the surfaces is several orders of magnitude slower. In purpose to realize the self-sustaining magnetically confined plasma, the discharged fusion energy has to heat the plasma. The energy produced in a fusion reaction is dispersed as kinetic energy to the fusion products.

2.5 DUSTY PLASMA PRODUCTION

We can produce dusty plasmas in laboratories using a number of techniques as explained below:-

2.5.1 MODIFIED Q-MACHINE

The dusty-plasma device is basically a single-ended *Q*-machine modified to allow the dispersal of dust-grains over a portion of the cylindrical-plasma column. A schematic diagram of the DPD is shown in figure(2.3). Single-ionized potassium-plasma is generated through ionization of potassium atoms on a hot tantalum plate which also serves as the source of thermionic electrons. Plasma is radially confined by longitudinal magnetic-field which measures up to about 0.35T. The electrons & ions are in thermodynamic-equilibrium with the hot plate having temperatures $T_e \approx T_i \approx 0.2$ eV [5].

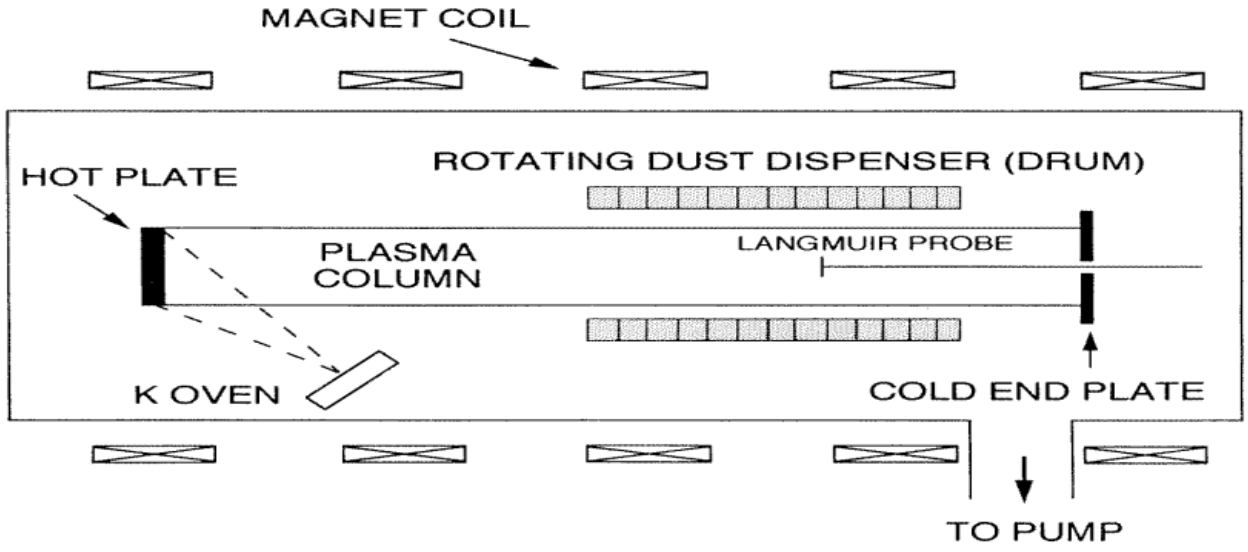

Figure (2.3): Schematic drawing of the dusty plasma device consisting of a *Q* - machine and rotating drum dust dispenser [37].

2.5.2 DUST IN DC & RF DISCHARGES

Discharges are used to produce plasmas for various purposes. For example, in processing silicon-wafers which are used in the manufacture of microchips or depositing shiny-coatings onto crisp packets, in home in the form of a fluorescent-light or in specially designed academic experiments.

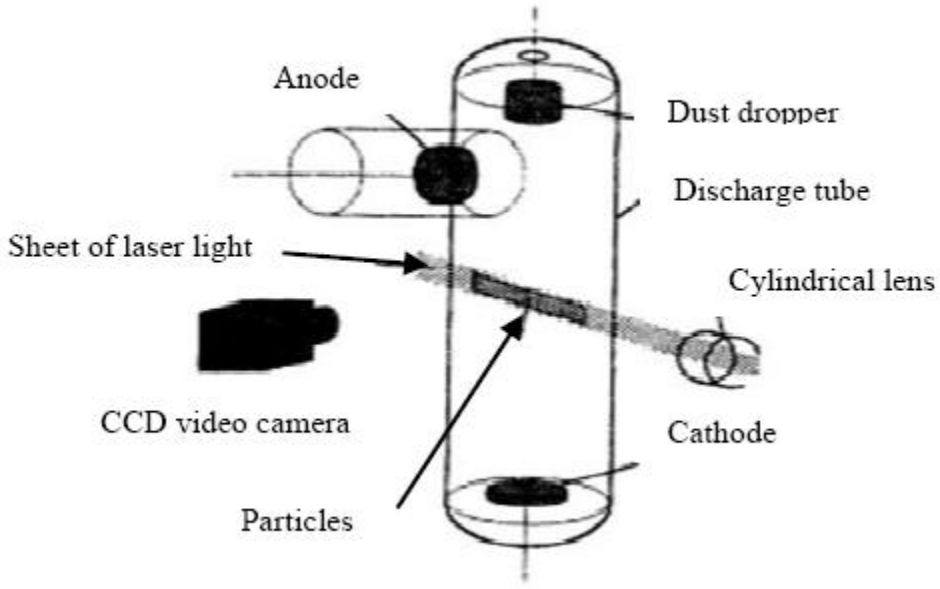

Figure 2.4: Schematic illustration of how dusty plasmas are produced in strata of a D.C. neon glow discharge [41].

Discharges may either be DC (example: fluorescent-lights), or RF with AC frequency usually at 13.56MHz. Plasma is generated inside a container where electrodes are arranged in a fashion to suit the purpose of discharge. A simple capacitive-discharge circuitry is shown in figure (2.4).

When it comes to plasma-processing, discharges have got a wide-range of applications. IC (integrated circuits) production incorporates repeated stages of deposition, masking, etching & stripping to make circuit-elements like transistors & capacitors. Production of such chips can be obtained from a small silicon-wafer. The place where such fabrications are done is usually dust-free zone. However, sputtering-events may still produce dust-particles which may ruin the process. Etching events are facilitated by placing substrate on a biased-electrode to accelerate ions in plasma. Specific ion-species can be selected to react with substrate to enhance etching, and because of this reason Cl & F-ions are used as they are highly reactive. Re-deposition technique is used to obtain thin film coatings. Here, the film-material is placed on the biased-electrode to enhance sputtering and then ions are directed onto the substrate by other electrodes. Sputtering being an un-predictable process produces dust as well as ions.

It is generally observed that dust is generated in both rf & dc discharges, but RF produces significantly more dust which are usually sub-micron size, and are unwanted by-product.

RF-discharges are frequently used in custom-made dusty-plasma experiments. They generally involve especially generated dust such that their sizes are closely monitored. The behavior of dust is of great interest since the discovery of dusty plasma crystals formation during experiments. On Earth, the discharge is directed vertically, the dust is generally levitated in sheath-area above the lower-electrode, as gravity is significant. However, there are some experiments being conducted in International Space Station where they produce microgravity condition, and the dust fill the whole discharge, excluding an eye-shaped void at the centre. The void is considered to be a result of the potential-distribution in the discharge. HCP(Hexagonal-close-packed) & BCC(body-centered-cubic) structures was observed both on Earth & in micro-gravity but the interaction between the dust-grains is poorly understood, though the analysis in most experiments assumes a Debye-Huckel repulsive-potential around each dust-grain. Many in the scientific community also think that an attractive-force between dust grains exists. It is therefore extremely hard to design experiments to peep at the potential-profile between the two grains because of the fact that diagnostics such as Langmuir-probes alter the plasma.

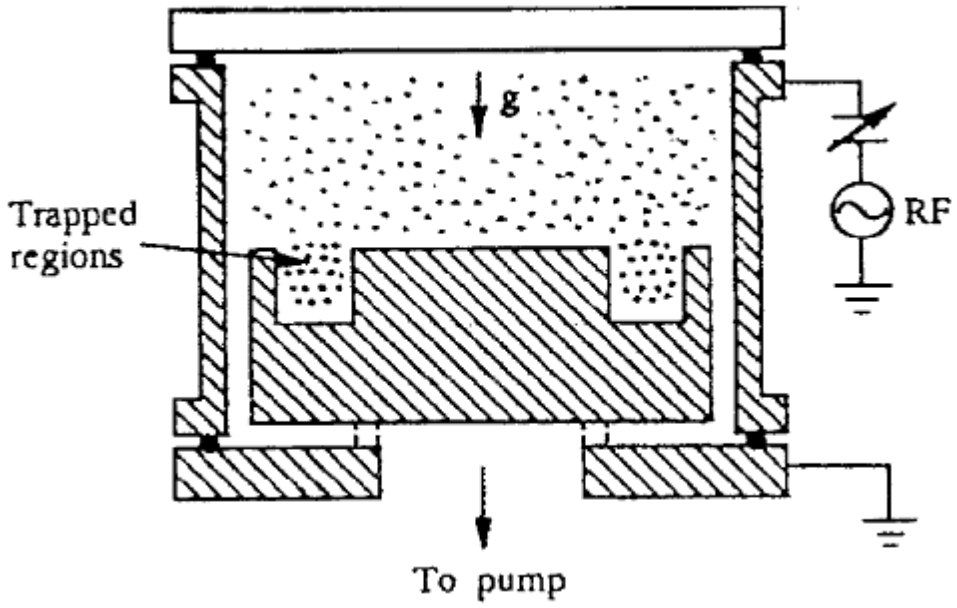

Figure (2.5): Side view of the cylindrical discharge system [38].

The kinetic-behaviour of the phase change of coupled dust-systems can be observed by changing the pressure of the neutral-gas in the rf-discharge, and hence, the amount of ionization. This diminishes charge on each dust-grain, and thereby the electrostatic-coupling, even though the

temperature of the dust remains same. The thermal-motion overcomes the electrostatic-forces, and liquid & gaseous phase can be obtained.

2.6 DUST CHARGING MECHANISMS

The elementary-processes which help in the charging of dust-grains are complex and mainly depend on the environment around the dust-grains. Some important primary dust-grain charging methods are [5]:-

(i) Interaction of dust grain with gaseous plasma particles,

(ii) Interaction of dust grains with energetic electrons and ions, and

(iii) Interaction of dust grains with photons

When the dust-grains are introduced in gaseous-plasma, the plasma-particles (electrons & ions) are collected by the dust-grains that act as probes. The dust-grains are, hence, charged by the collection of the plasma-particles flowing onto their surface.

2.7 ROLE OF DUST IN TOKAMAK

As we know that in magnetic-confinement of fusion devices, small particles exist [33], for instance if after some time of operation of tokamak, its bottom area is cleaned, one can collect fine grain materials. On wiping fusion device because of dust consequences on the device & its thermonuclear which need to be addressed are just the beginnings [34]. The safety aspects related to plasma-operation & its performance and thus the safety of the thermonuclear fusion reactor can be easily distinguished. Works related to the 1^{st} aspect has gained whereas about the 2^{nd} aspect; practically nothing is known. Inventory of a dust-concern about the reactor's safety in future. Since dust-bound tritium is not reprocessing-loop hence, it increases the inventory of the site. In case of a severe accident, dust may also become a vehicle making tritium mobile. An explosion hazard can be considered as further aspect which can exist when gushing out steam from it can combine with oxygen in the environment to form an explosive-mixture.

CHAPTER 3

LITERATURE REVIEW

3.1: INTRODUCTION

The past decade of research in plasma confinement has shown that plasma transport across the magnetic field is largely controlled by low frequency drift wave fluctuations [12]. The purpose of study various research to describe the fast wave stabilization and destabilization of drift wave in a plasma with dust grain. The area of research is rich with many theoretical and computational tools and laboratory experiments developed over the past several decades in the magnetic fusion energy research programs throughout the world. The present review necessarily selects a small fraction of the information currently available about the role of low frequency drift wave fluctuations and the associated plasma transport in magnetized plasmas and stabilization and destabilization of drift wave in plasma [31].

Kumar and Tripathi[31],have described Four wave-nonlinear coupling of a large amplitude whistler with low frequency drift wave and whistler wave sidebands is examined. The pump and whistler sidebands exert a low frequency ponderomotive force on electrons introducing a frequency shift in the drift wave. For whistler pump propagating along the ambient magnetic field $B_s\hat{z}$ with wave number $\vec{k}_0$ drift waves of wave number $\vec{k} = \vec{k}_\perp + k_\parallel \hat{z}$ see an upward frequency shift when $k_\perp^2 / k_0^2 > 4k_\parallel / k_0$ and are stabilized once the whistler power exceeds a threshold value. The drift waves of low transverse wavelength tend to be destabilized by the nonlinear coupling. Oblique propagating whistler pumps with transverse wave vector parallel to $\vec{k}_\perp$ is also effective but with reduced effectiveness.

Kuley and Tripathi[30],have described, Parametric coupling of lower hybrid pump wave with low frequency. Collision less/weakly collision trapped electron drift wave, with frequency lower than the electron bounce frequency, is studied. The coupling produces two lower hybrid sidebands. The sidebands beat with the pump to exert a low frequency ponderomotive force on electrons that causes a frequency shift in the drift wave, leading to the growth of the latter. The short wavelength modes are destabilized and they enhance the anomalous diffusion coefficient.

Horton [8], has study, Drift waves occur universally in magnetized plasmas producing the dominant mechanism for the transport of particles, energy and momentum across magnetic field lines. A wealth of information obtained from quasistationary laboratory experiments for plasma confinement is reviewed for drift waves driven unstable by density gradients, temperature gradients and trapped particle effects. The modern understanding of Bohm transport and the role of sheared flows and magnetic shear in reducing the transport to the gyro-Bohm rate are explained and illustrated with large scale computer simulations. The types of mixed wave and vortex turbulence spontaneously generated in nonuniform plasmas are derived with reduced magnetized fluid descriptions. The types of theoretical descriptions reviewed include weak turbulence theory, Kolmogorov anisotropic spectral indices, and the mixing length. A number of

standard turbulent diffusivity formulas are given for the various space-time scales of the drift wave turbulent mixing.

Hooke et al. [10], have study, Electro-statically driven oscillations near the lower-hybrid-resonance frequency have been studied in a linear plasma device. The index of refraction of these waves is measured directly and is seen to peak at a critical density as the wave propagates radially inward. A strong, nonlinear interaction is observed between the driven oscillations and the low-frequency drift-wave-like fluctuations which exist in this plasma.

Hendel et al.[9], have study, Density-gradient-driven collisional drift waves are identified by the dependences of ω and **k** on density, temperature, magnetic field, and ion mass, and by comparisons with a linear theory which includes resistivity and viscosity. Abrupt stabilization of azimuthal modes is observed when the stabilizing ion diffusion over the transverse wavelength due to the combined effects of ion Larmor radius and ion-ion collisions (viscosity) balances the destabilizing electron-fluid expansion over the parallel wavelength, determined by electron-ion collisions (resistivity). The finite-amplitude ($\tilde{u}/n_0 \simeq 10\%$) coherent oscillation, involving the entire plasma body, shows a phase difference between density and potential waves (which is predicted by linear theory for growing perturbations). The wave-induced radial transport exceeds classical diffusion, but is below the Bohm value by an order of magnitude. Although observations have been extended to magnetic fields three times those for drift-wave onset, turbulence has not been encountered.

Satya et al[11],have described, The influence of a turbulent spectrum of high-frequency, short-wavelength electron plasma waves on the linear dispersion relation for low-frequency, long-wavelength drift waves has been analytically investigated.

Liu,et al[13],have obtained, The drift-wave instability due to an electron temperature gradient opposite to the density gradient is analyzed as a possible explanation for the observed anomalous skin effect in tokamaks.

Horton [14], has described, An expression for the spectral distribution of drift-wave fluctuations is obtained from a new mode-coupling equation that describes the superposition of drift-wave normal modes induced by the divergence of the nonlinear E×B convective flux. Computations for the adiabatic toroidal compressor experiment indicate that the observed spectrum is consistent with the theoretical spectrum.

Ross et al.[15], have described, It is shown that the eigenmodes of the collisionless drift wave in slab geometry are stable. Previous studies yielding instability (the "universal" instability) were based upon an incomplete treatment of the electron dynamics; i.e., the principal part of the plasma dispersion function was ignored.

Callen [16] has obtained, The small magnetic perturbations accompanying drift waves are shown to produce microscopic, fluctuating magnetic island structures and to enhance radial electron heat transport in tokamaks. The "magnetic-flutter"-induced electron heat-conduction coefficient is found to be $\chi_e^{\delta} \simeq 3/16\,(\nu+\gamma)\delta^2$ where δ is the magnetic island width, ν is the

electron-ion collision frequency, and γ is the drift-wave growth rate, or inverse island correlation time.

Lee et al.[17]have described, The collisionless drift wave and drift-Alfvén wave instabilities in a sheared magnetic field are considered using the complex transformation technique of Antonsen. It is shown that no unstable bounded eigensolutions for the finite-β radial eigenmode equations exist. We also present a more general technique based on the wave-flux conservation and find, furthermore, that the convective amplification of drift waves in the electrostatic limit can be anomalously large, which could lead to enhanced transport in tokamaks.

Nishida et al.[19], have *described,* The suppression of drift instability is observed by applying a homogeneous rf electric field in a dc discharge diffused plasma. The instability amplitude is reduced by more than a factor of 30 and, concomitantly, a decrease of plasma loss across the magnetic field is also observed.

Hasegawa,[18] has obtained, While the ordinary electrostatic drift mode is stabilized by either high-β effects or an admixture of cold plasma, a compressional drift mode is shown to be destabilized under these same circumstances. The condition of the instability is approximately given by $\frac{n_h}{n_c} < \beta\kappa_0^2\rho_i^2$ where n_h and n_c are the number densities of the hot and cold components, respectively κ_0 is a measure of the density, temperature, or magnetic field gradients; and ρi is the ion Larmor radius.

Alcock et al.[20],have study, Experimental results are presented which show the stabilization of the drift-dissipative instability in an afterglow plasma. Stabilization was achieved by means of an applied azimuthal rf magnetic field perpendicular to the main containing axial magnetic field or, alternatively, by an applied rf axial electric field parallel to the dc magnetic field. The results obtained at various applied frequencies are compared with a previous theory, and some points of agreement and disparity are noted.

Sen et al.[21], have described, The use of radio frequency waves is shown to stabilize drift-type waves in a tokamak if the radial profile of the radio frequency field energy is properly chosen. The estimate of the radio frequency power required for this stabilization is found to be rather modest. This result m*e et al.[22], described* Stabilization of drift waves by external rf fields at frequencies near the lower-hybrid frequency has been observed experimentally in a Q machine in the collisionless regime with $\left(\frac{\omega_{pe}}{\omega_{ce}}^2\right)^2 \ll 1$ Stabilization is due to a resonant ponderomotive force which increases the drift frequency, thus enhancing the electron Landau damping. The observations are in general accord with analyses in the literature when finite-geometry effects appropriate to the present experiment are taken into account.

Liu et al.[23], have described, The lower hybrid waves of finite wave number k_0 are shown to be able to quench the entire k spectrum of unstable drift waves in tokamak plasmas for k_0 greater than k, where k_0 is perpendicular to k. In relatively cold plasmas, where k_0 may become less than

k, one needs to invoke the ion damping to stabilize the whole spectrum. The analysis explains very well the experimental results of Gore, Grun, and Lashinsky on the suppression of whole drift wave spectrum in a *Q* machine by a lower hybrid electric field.

Kuley and Tripathi[24],have described, A gyrokinetic formalism has been developed to study lower hybrid wave stabilization of ion temperature gradient driven modes, responsible for anomalous ion transport in the inner region of tokamak. The parametric coupling between lower hybrid and drift waves produce lower hybrid sideband waves. The pump and the sidebands exert a ponderomotive force on electrons, modifying the eigenfrequency of the drift wave and influencing the growth rate. The longer wavelength drift waves are destabilized by the lower hybrid wave while the shorter wavelengths are suppressed. The requisite lower hybrid power is in the range of ~900 kW at 4.6 GHz.

DuBois,et al.[25], have described, In magnetically confined fusion plasmas, drift wave driven turbulence can lead to enhanced particle transport from the plasma. Because of this, a significant research emphasis has been placed on the suppression of drift waves in the plasma edge. However, the combination of the toroidal geometry and short plasma lifetimes can make it difficult to fully characterize the properties of these instabilities. Because linear magnetized plasma devices offer a combination of simpler geometry and steady state plasma generation, it is possible to perform detailed studies of many types of plasma instabilities including drift waves. This paper reports on a recent experiment in which low frequency instabilities ($\omega \leq \omega ci$) in the Auburn Linear Experiment for Instability Studies plasma device were characterized as drift waves and through changes in the parallel current, it is shown that it is possible to suppress these instabilities.

Liu and Tripathi[27],have described, A general formalism of parametric instabilities of electrostatic and electromagnetic waves in a magnetized plasma is presented. The Vlasov equation has been solved in the guiding center variables, incorporating the effects of finite wave number of pump, finite Larmor radius, resonant wave-particle interaction, and diamagnetic drift. In the limit of small Larmor radius, drift kinetic equation provides a simpler description. When applicable, fluid theory is used to yield a clearer physical picture. Only when the decay waves have wavelengths much shorter than that of the pump, the dipole pump ($k_0 = 0$) approximation usually employed, is valid and the coupling coefficient, including full kinetic effects on the decay waves, is expressible in terms of electron and ion susceptibilities. The scheme adopted here is applicable to laboratory experiments as well as space plasma.

Sharma et al. [28], have described, A spiraling ion beam propagating through a magnetized dusty plasma cylinder drives electrostatic ion cyclotron waves to instability via cyclotron interaction. Numerical calculations of the growth rate and unstable mode frequencies have been carried out for the typical parameters of dusty plasma experiments in the two limits, namely, long parallel wavelength and short parallel wavelength. It is found that as the density ratio of negatively charged dust grains to electrons increases, the unstable mode frequency and the growth rate of the instability of the ion cyclotron waves increase in both the limits. The growth rate of the instability increases by a factor of ~2.5 when the density ratio of negatively charged dust grains changes from 1.0 to 4.0 in the limit of short parallel wavelengths. Moreover, the growth rate increases with the density ratio of negatively charged dust at higher values in the present case in

the limit of long parallel wavelengths. The growth rate of the unstable mode has the largest value for the modes whose eigenfunctions peak at the location of the beam. The growth rate of the instability scales as the one-third power of the beam current in both limits.

Sharma et al. [29], have obtained, An electron beam propagating through a magnetized dusty plasma drives electrostatic lower hybrid waves to instability via Cerenkov interaction. A dispersion relation and the growth rate of the instability for this process have been derived taking into account the dust charge fluctuations. The frequency and the growth rate of the unstable wave increase with the relative density of negatively charged dust grains. Moreover, the growth rate of the instability increases with beam density and scales as the one-third power of the beam density. In addition, the dependence of the growth rate on the beam velocity is also discussed.

Kumar and Tripathi[32] have described, The parametric coupling of a high amplitude lower hybrid wave with the ion cyclotron instability, driven by neutral beam converted ion beam, is studied. The coupling is strong when the wave numbers of the pump and the ion cyclotron wave are perpendicular to each other; it produces lower hybrid sidebands. When the upper sideband is resonant, the growth rate of the instability is suppressed as the energy is fed into the upper sideband by the pump and the ion cyclotron wave. At different wave numbers when the lower sideband is resonant, the parametric coupling leads to the enhancement of growth rate. The effect is important when electron quiver velocity is greater than the sound speed. The study is relevant to advanced stage operations of a tokamak like ITER.

CHAPTER 4

MATHEMATICAL MODELING

4.1 INTRODUCTION

Drift waves are a matter of concern in magnetically confined plasmas, e.g., tokamak.[7][15]. It contributes in enhanced molecule transport over the magnetic field [16][18]. Endeavors have been made to balance out them by the utilization of radio frequency (rf) handle in the lower hybrid frequency [19][21] and analyzed the whole spectra of drift waves in Q-machine[22] and built up a hypothetical frame work and clarified these outcomes as a four-wave parametric coupling[23]. The rf pump beats with small frequency drift wave making nonlinear thickness irritations that drive two lower hybrid sidebands. The sidebands and pump apply a contemplate thought process constrain on electrons stifling the drift wave as of late concentrated on the nonlinear coupling of lower hybrid wave with the temperature inclination driven modes utilizing a motor formalism[24]. They found that the ponderomotive force applied on electrons by the pump and sidebands adjusted the eigen frequency of the drift wave. The more extended wavelength drift waves are destabilized by the lower hybrid wave, while shorter wavelengths are smothered and watched the concealment of drift waves in direct polarized plasma segment through blend of radial electric field with transverse and parallel streams [25].

We read about the nonlinear 4-wave coupling of a huge magnitude whistler with the low frequency drift waves. The drift waves have parallel wave vector practically opposite to the magnetic field and thickness inclination; on the other hand, parallel phase velocity (along the field lines) is much littler than the thermal speed. The limited Larmor range impact causes their destabilization. In the vicinity of an extensive sufficiency whistler, the electrons obtain an E×Bdrift. The float speed beats with the electron thickness annoyance because of the float wave to deliver nonlinear streams amid the lower and upper sideband whistler waves. The last couples with the pump to apply a parallel ponderomotive drive on electrons bringing on a recurrence move in the float wave. Drift waves of shorter opposite wavelengths endure an upward frequency shift and have a tendency to be balanced out while the ones of longer wavelengths have a tendency to get destabilized [31].

We add to the formalism of four waves coupling to drift waves with whistler pump spreading along the surrounding magnetic fields with dust grain in plasma.

4.2 STABLIZATION AND DESTALIZATION ANALYSIS

Following the analysis of Kumar and Tripathi [31], the electrostatic potential

$$\phi = A\exp\left[-i\left(\omega t - k_{\perp} y - k_z \hat{z}\right)\right] \tag{4.1}$$

Let consider electron and ion densities $n(x)$ in an inhomogeneous plasma where immerged in static magnetic field $B_0\hat{z}$. The electron and ion having temperatures T_e and T_i in process of diamagnetic drifts [31]-

$$\begin{aligned} \vec{v}_{ed} &= -y\frac{v_{the}^2}{\omega_{ce}L_n} \\ \vec{v}_{id} &= +y\frac{v_{thi}^2}{\omega_{ci}L_n} = -\vec{v}_{ed}\frac{T_i}{T_e}, \end{aligned} \tag{4.2}$$

where

$v_{the} = \left(\frac{T_e}{m_{0e}}\right)^{1/2}$, $v_{thi} = \left(\frac{T_i}{m_{0i}}\right)^{1/2}$, $\omega_{ce} = -\frac{eB_0\hat{z}}{m_{0e}}$, $\omega_{ci} = \frac{eB_0\hat{z}}{m_{0i}}$ and $L_n = (1/n)\frac{\partial n}{\partial x}$ is the density scale length, -e and m_{0e} are the electronic charge and mass of electron, m_{0i} is mass of ion.

In the plasma, we launch a large amplitude whistler, propagating along $B_0\hat{z}$ with right handed circular polarization.[31]

$$\begin{aligned} \vec{E}_{0n} &= A_{0n}\left(\hat{x} + i\hat{y}\right)\exp\left[-i\left(\omega_{0n}t - k_n\hat{z}\right)\right] \\ \vec{B}_{0n} &= \frac{\vec{k}_{0n}\times\vec{E}_{0n}}{\omega_{0n}} \end{aligned} \tag{4.3}$$

where we choose $\omega_m << \omega_{ci}$. The whistler provides oscillatory velocity of electrons-

$$\vec{v}_{0e} = \frac{e\vec{E}_{0n}}{im\left(\omega_{0n} - \omega_c\right)} \approx \frac{e\vec{E}_{0n}}{im\omega_c} \tag{4.4}$$

The drift velocity beats with the low frequency electron density perturbation n_{1e} to produced non linear current densities at $\omega_1 = \omega - \omega_0, \vec{k}_1 = \vec{k} - \vec{k}_0$, and $\omega_2 = \omega + \omega_0, \vec{k}_2 = \vec{k} + \vec{k}_0$ [31]

$$\begin{aligned} \vec{J}_{x1}^{NL} &= -\frac{1}{2}n_{1e}e\vec{v}_{0e}^{*} \\ \vec{J}_{x2}^{NL} &= \frac{1}{2}n_{1e}e\vec{v}_{0e} \end{aligned} \tag{4.5}$$

Here we have used the identity-

$$\langle Re\rangle \vec{A}.\langle Re\rangle \vec{B} = (1/2)\langle Re\rangle\left[\vec{A}.\vec{B} + \vec{A}^{*}.\vec{B}\right],$$

where <Re> denotes the real part of quantity and * implies the complex conjugate.

The current driven the whistler wave sideband with electric and magnetic fields-[31]

$$\vec{E}_{jn} = A_{jn}\left(\hat{x} + \beta'_{jn} i\hat{y}\right)\exp\left[-i\left(\omega_j t - \vec{k}_n \vec{r}\right)\right],$$
$$\vec{B}_{jn} = \frac{\vec{k}_{jn} \times \vec{E}_{jn}}{\omega_{jn}}, \tag{4.6}$$

where j=1,2 and $\vec{k}_1 = \vec{k}_\perp \hat{y} + (k_z - k_0)\hat{z}$, $\vec{k}_2 = \vec{k}_\perp \hat{y} + (k_z + k_0)\hat{z}$

The wave equation governing $\vec{E}_{1n}$ in the absence of the pump is-

$$\nabla^2 \vec{E}_{1n} - \nabla\left(\nabla \cdot \vec{E}_{1n}\right) + \frac{\omega_1^2}{c}\vec{\vec{\varepsilon}}_{1n} \cdot \vec{E}_{1n} = 0 \tag{4.7}$$

Replacing ∇ by $i\vec{k}_{jn}$ in Eq.(4.7) gives-

$$k^2 \vec{E}_0 - \left(k.\vec{E}_0\right)k - \frac{\omega_1^2}{c^2}\vec{\vec{\varepsilon}}_{1n} \cdot \vec{E}_{1n} = 0$$

$$\vec{\vec{D}}_{1n} \cdot \vec{E}_{1n} = 0 \tag{4.8}$$

where

$$\vec{\vec{D}}_{1n} = \varepsilon_{1n} - \frac{k_1^2 c^2}{\omega_1^2} - \frac{c^2}{\omega_1^2}\vec{k}_1\vec{k}_1 \tag{4.9}$$

and $\varepsilon_{1xx} = \varepsilon_{1yy} = 1 - \frac{\omega_p^2}{\omega_1^2 - \omega_c^2} \approx 1 + \frac{\omega_p^2}{\omega_1^2}$, $\varepsilon_{1xy} = -\varepsilon_{1yx} = i\frac{\omega_c}{\omega_1}\frac{\omega_p^2}{\omega_1^2 - \omega_c^2} \approx -i\frac{\omega_p^2}{\omega_1^2 \omega_c}$,

$\varepsilon_{1zz} = 1 - \frac{\omega_p^2}{\omega^2} \approx -\frac{\omega_p^2}{\omega^2}$, $\varepsilon_{1xy} = \varepsilon_{1zy} = \varepsilon_{1zx} = 0$

where $\omega_p = \left(\frac{n_0^0 e^2}{m\varepsilon_0}\right)^{1/2}$ is plasma frequency and ε_0 is the free space permittivity.

The tensor (A scalar can be designated a tensor of rank zero) $\vec{\vec{\varepsilon}}$ nine components. Only under special circumstances, the tensor becomes Hermitian $\varepsilon_{ij} = \varepsilon_{ij}^{*}$, which is the condition for the absence of wave energy dissipation by the plasma.

The z- component of Eq.(4.8) reveals that in the limit $\omega_1 << \omega_c$, $E_{1nz}=0$ and $|D_{1n}|=0$ give the linear dispersion relation for lower sideband whistler-

$$k_1^2 k_{z1}^2 = \frac{\omega_p^4}{c^4}\frac{\omega_1^2}{\omega_c^2}, \tag{4.10}$$

The x-component of Eq.(4.8) gives

$$E_{1ny} = -\frac{D_{1nxx}}{D_{1nxy}}E_{1nx} = -\frac{\varepsilon_{1nxx} - k_{1z}^2/\omega_1^2}{\varepsilon_{1nxy}}E_{1nx}, \tag{4.11}$$

$$\beta'_{n1} = +i\left(k_{z1}/k_1\right)$$

Similarly for the upper side band-[31]

$$k_2^2 k_{z2}^2 = \frac{\omega_p^4}{c^4}\frac{\omega_2^2}{\omega_c^2}, \beta'_{n2} = +i\left(k_{z2}/k_2\right) \tag{4.12}$$

For $k_z << k_0$, $\beta'_{n1} = -i$ and $\beta'_{n2} = +i$

The sideband whistler provides oscillatory velocity of electrons-[31]

$$\vec{v}_{1e} = \frac{e\vec{E}_{1n}}{im\omega_c}, \vec{v}_{2e} = -\frac{e\vec{E}_{2n}}{im\omega_c} \tag{4.13}$$

and these velocities beat with the pump to exert low frequency pondermotive force $\vec{F}_p$. Here only consider the z-component of $\vec{F}_p$ as electron response to transverse pondermotive force is strongly inhibited by the magnetic field.

$$F_{pz} = -\frac{e}{2}\left(\vec{v}_{0e}\times\vec{B}_{1n}\right)_z - \frac{e}{2}\left(\vec{v}_{1e}\times\vec{B}_{0n}\right)_z - \frac{e}{2}\left(\vec{v}^*_{0e}\times\vec{B}_{2n}\right)_z - \frac{e}{2}\left(\vec{v}_{2e}\times\vec{B}^*_{0n}\right)_z$$

$$F_{pz} = ik_z e\phi_m \tag{4.14}$$

where-

$$\phi_m = +\frac{e}{m\omega_0\omega_c}\left(E_{x0}E_{n1x} + E^*_{x0}E_{n2x}\right) \tag{4.15}$$

The electron response to ϕ and ϕ_m in the limit of $\frac{\omega}{k_z v_{thi}} << 1$ can be adiabatic given as [27]-

$$n_{1e} = \frac{k^2 \varepsilon_0 \chi_{1e}}{e}\left(\phi + \phi_m\right) \tag{4.16}$$

where χ_{1e} is the electron susceptibility and its value [27]-

$$\chi_{1e} = \frac{\omega_{pi}^2}{k^2 c_s^2}\left[1 + i\sqrt{\pi}\,\frac{\omega - \omega_m^*}{k_z v_{the}}\right] \text{ and } \omega_m^* = \frac{k v_{the}^2}{\omega_c L_n} \tag{4.17}$$

The ion response can be taken to be linear [27]-

$$n_{1i} = -\frac{k^2 \varepsilon_0 \chi_{1i}}{e}\phi \tag{4.18}$$

where χ_{1i} is the ion susceptibility and its value is[27]-

$$\chi_{1i} = \frac{\omega_{pi}^2}{k^2 c_s^2}\left[\frac{T_e}{T_i} b_{1i} - \frac{\omega_m^*}{\omega}\left(1 - b_{1i}\right)\right] \tag{4.19}$$

4.3 DUST CHARGE CALCULATION

Now introduced the dust density n_{1D} immersed in a static magnetic field (**B**) in z-direction.

The dust density perturbation is given by-[28][29]

$$n_{1D} = -\frac{n_{0D} Q_{0D} k^2 \varepsilon_0 \phi}{m_{0D} \omega^2} \tag{4.20}$$

where

Q_{0D} is charge of dust, m_{0D} is mass of dust.

In the present case dust is consider unmagnetized because $\omega \sim \omega_{ci} >> \omega_{cD}$ with $\omega_{cD} = \frac{Q_{0D} B_0}{m_{0D}}$

where ω_{cD} is dust gyro-frequency.

Now we applying probe theory for dust grain, the charge of dust grain Q_D is known to be balanced with the plasma currents on the dust grain surface as [42]-

$$-\frac{Q_D}{dt} = I_{1e} + I_{1i} \tag{4.21}$$

The dust charge fluctuation is governed by the equation-

$$\frac{Q_{1D}}{dt} + \eta Q_{1D} = -|i_{e0}|\left(\frac{n_{1i}}{n_{0e}} - \frac{n_{1e}}{n_{0e}}\right) \tag{4.22}$$

where-

$$\eta = \frac{|I_{0e}|e}{C_g}\left[\frac{1}{T_e} + \frac{1}{T_i - e\phi_{0g}}\right] \tag{4.23}$$

$Q_{1D} = Q_D - Q_{0D}$ is the perturbed dust grain charge,

$C_g = a\left(1 + \frac{a}{\lambda_{eD}}\right)$ is the capacitance of the dust grain, a is the dust grain size and λ_{eD} is the electron Debye length.

Substituting $d/dt = -i\omega$ in Eq. (4.22), we obtain the dust charge fluctuation Q_{1D} -

$$Q_{1D} = -\frac{|i_{0e}|}{i(\omega + i\eta)}\left(\frac{n_{1i}}{n_{0i}} - \frac{n_{1e}}{n_{0e}}\right) \tag{4.24}$$

By putting the value of n_{1e} and n_{1i} in Eq.(4.24) from Eq.(4.16) and (4.18) we get-

$$Q_{1D} = \frac{i|i_{e0}|}{(\omega + i\eta)}\left(-\frac{\frac{k^2\varepsilon_0(1+\chi_{1i})}{e}\phi}{n_{0i}} - \frac{\frac{k^2\varepsilon_0\chi_{1e}}{e}(\phi + \phi_m)}{n_{0e}}\right)$$

$$Q_{1D} = \frac{i|i_{e0}|}{(\omega + i\eta)}\left(-\frac{k^2\varepsilon_0(1+\chi_{1i})\phi}{en_{0i}} - \frac{k^2\varepsilon_0\chi_{1e}(\phi + \phi_m)}{en_{0e}}\right)$$

$$Q_{1D} = \frac{i|i_{e0}|}{n_{0e}(\omega + i\eta)}\left(-\frac{n_{0e}}{n_{0i}}\frac{k^2\varepsilon_0(1+\chi_{1i})\phi}{e} - \frac{k^2\varepsilon_0\chi_{1e}(\phi + \phi_m)}{e}\right)$$

$$Q_{1D} = \frac{i|i_{e0}|}{n_{0e}(\omega + i\eta)}\left(-\frac{n_{0e}}{n_{0i}}\frac{k^2\varepsilon_0\phi}{e}\chi_{1i} - \frac{k^2\varepsilon_0\chi_{1e}}{e}\phi - \frac{k^2\varepsilon_0\chi_{1e}}{e}\phi_m\right)$$

$$Q_{1D} = -\frac{i|i_{e0}|}{n_{0e}(\omega + i\eta)}\left(\frac{n_{0e}}{n_{0i}}\frac{k^2\varepsilon_0\phi}{e}\chi_{1i} + \frac{k^2\varepsilon_0\chi_{1e}}{e}\phi + \frac{k^2\varepsilon_0\chi_{1e}}{e}\phi_m\right) \tag{4.25}$$

Eq.(4.25) is dust charge fluctuation.

Using Eq.(4.16),(4.18),(4.20)and (4.25) in the poisson's equation-

$$\nabla^2\phi = \frac{e}{\varepsilon_0}\left(n_{1e} - n_{1i} - n_{oD}Q_{1D} - Q_{oD}n_{1D}\right), \text{ we get-}$$

$$\nabla^2\phi = \frac{e}{\varepsilon_0}\left[\frac{k^2\varepsilon_0\chi_{1e}}{e}(\phi + \phi_m) + \frac{k^2\varepsilon_0\chi_{1i}}{e}\phi + \frac{n_{0D}i|i_{e0}|}{n_{0e}(\omega + i\eta)}\left(\frac{n_{0e}}{n_{0i}}\frac{k^2\varepsilon_0\phi}{e}\chi_{1i} + \frac{k^2\varepsilon_0\chi_{1e}}{e}\phi + \frac{k^2\varepsilon_0\chi_{1e}}{e}\phi_m\right) + Q_{0D}\frac{n_{0D}Q_{0D}k^2\varepsilon_0\phi}{m_{0D}\omega^2}\right]$$

$$\nabla^2\phi = \frac{e}{\varepsilon_0}\left[\frac{k^2\varepsilon_0\chi_{1e}}{e}\phi + \frac{k^2\varepsilon_0\chi_{1e}}{e}\phi_m + \frac{k^2\varepsilon_0\chi_{1i}}{e}\phi + \frac{n_{0D}i|i_{e0}|}{n_{0e}(\omega + i\eta)}\frac{n_{0e}}{n_{0i}}\frac{k^2\varepsilon_0\phi}{e}\chi_{1i} + \frac{n_{0D}i|i_{e0}|}{n_{0e}(\omega + i\eta)}\frac{k^2\varepsilon_0\chi_{1e}}{e}\phi + \frac{n_{0D}i|i_{e0}|}{n_{0e}(\omega + i\eta)}\frac{k^2\varepsilon_0\chi_{1e}}{e}\phi_m + \frac{n_{0D}Q_{0D}^2k^2\varepsilon_0\phi}{m_{0D}\omega^2}\right]$$

put $\nabla^2 = -k^2$

$$-k^2\phi = \frac{k^2\varepsilon_0 e}{\varepsilon_0}\left[\frac{\chi_{1e}}{e}\phi + \frac{\chi_{1e}}{e}\phi_m + \frac{\chi_{1i}}{e}\phi + \frac{i|i_{e0}|}{n_{0e}(\omega + i\eta)}\frac{n_{0e}}{n_{0i}}\frac{\phi}{e}\chi_{1i} + \frac{i|i_{e0}|}{n_{0e}(\omega + i\eta)}\frac{\chi_{1e}}{e}\phi + \frac{i|i_{e0}|}{n_{0e}(\omega + i\eta)}\frac{\chi_{1e}}{e}\phi_m + \frac{n_{0D}Q_{0D}^2\phi}{m_{0D}\omega^2}\right]$$

$$-\phi = \left[\chi_{1e}\phi + \frac{i\beta}{(\omega + i\eta)}\chi_{1e}\phi + \chi_{1i}\phi + \frac{i\beta}{(\omega + i\eta)}\frac{n_{0e}}{n_{0i}}\chi_{1i}\phi + \chi_{1e}\phi_m + \frac{i\beta}{(\omega + i\eta)}\chi_{1e}\phi_m + \frac{\omega_{pD}^2\phi}{\omega^2}\right]$$

$$-\phi = \chi_{1e}\phi\left(1 + \frac{i\beta}{(\omega + i\eta)}\right) + \chi_{1i}\phi\left(1 + \frac{i\beta}{(\omega + i\eta)}\frac{n_{0e}}{n_{0i}}\right) + \chi_{1e}\phi_m\left(1 + \frac{i\beta}{(\omega + i\eta)}\right) + \chi_d\phi$$

$$-\phi = \chi'_{1e}\phi + \chi'_{1i}\phi + \chi'_{1e}\phi_m + \chi_d\phi$$

$$-\phi(\chi'_{1e}+\chi'_{1i}+\chi_d)=\chi'_{1e}\phi_m$$

$$\varepsilon'\phi=-\chi'_{1e}\phi_m \tag{4.26}$$

where

$\varepsilon'=\chi'_{1e}+\chi'_{1i}+\chi_d$ Dispersion relation with dust.

$\omega_{pD}=\left(\frac{n_{0D}Q_{0D}^2}{m_{0D}}\right)^{1/2}$ is dust plasma frequency.

$\beta=\frac{n_{oD}|I_{0e}|}{en_{oe}}$ is coupling factor and it gives $\beta=0.397\left(1-\frac{1}{\delta}\right)\left(\frac{a}{v_{the}}\right)\omega_{pi}^2\left(\frac{m_{0i}}{m_{0e}}\right)$ and $\delta=\frac{n_{0i}}{n_{0e}}$

$\chi'_{1e}=\chi_{1e}\left[1+\frac{i\beta}{(\omega+i\eta)}\right]$ is dust included electron susceptibility.

$\chi'_{1i}=\chi_{1i}\left[1+\frac{i\beta}{(\omega+i\eta)}\frac{n_{0e}}{n_{0i}}\right]$ is dust included ion susceptibility.

One may also write n_{1e} explicitly in term of ϕ [31]-

$$\mathrm{n_{1e}}=-\frac{\mathrm{k}^2\varepsilon_0}{\mathrm{e}}(1+\chi_{1\mathrm{i}})\phi \tag{4.27}$$

Using the value of $\mathrm{n_{1e}}$ in Eq.(4.5) then obtained sideband current densities [31]-

$$\vec{\mathrm{J}}_{\mathrm{x1}}^{\mathrm{NL}}=-\frac{\mathrm{k}^2\varepsilon_0}{\mathrm{e}}(1+\chi_{1\mathrm{i}})\phi\frac{\mathrm{eE}_{\mathrm{x0}}^*(\hat{\mathrm{x}}-\mathrm{i}\hat{\mathrm{y}})}{\mathrm{im}\omega_{\mathrm{c}}}$$

$$\vec{\mathrm{J}}_{\mathrm{x2}}^{\mathrm{NL}}=-\frac{\mathrm{k}^2\varepsilon_0}{\mathrm{e}}(1+\chi_{1\mathrm{i}})\phi\frac{\mathrm{eE}_{\mathrm{x0}}^*(\hat{\mathrm{x}}+\mathrm{i}\hat{\mathrm{y}})}{\mathrm{im}\omega_{\mathrm{c}}} \tag{4.28}$$

Using these current densities in the wave equation-

$$\nabla^2\vec{\mathrm{E}}_{\mathrm{nj}}-\nabla\left(\nabla\cdot\vec{\mathrm{E}}_{\mathrm{nj}}\right)+\frac{\omega_1^2}{\mathrm{c}}\vec{\varepsilon}_{\mathrm{nj}}\cdot\vec{\mathrm{E}}_{\mathrm{nj}}=-\frac{\mathrm{i}\omega_{\mathrm{j}}}{\mathrm{c}^2\varepsilon_0}\vec{\mathrm{J}}_{\mathrm{xj}}^{\mathrm{NL}} \tag{4.29}$$

Replacing ∇ by $\mathrm{i}\vec{\mathrm{k}}_{\mathrm{j}}$ in Eq.(4.27) gives

$$\vec{\mathrm{D}}_{\mathrm{nj}}\cdot\vec{\mathrm{E}}_{\mathrm{nj}}=-\frac{\mathrm{i}\vec{\mathrm{J}}_{\mathrm{xj}}^{\mathrm{NL}}}{\omega_{\mathrm{j}}\varepsilon_0} \tag{4.30}$$

where j=1,2 and D_1 is defined in Eq.(4.9) and D_2 may be recovered from replacing ω_1 by ω_2 and $\vec{k}_1$ by $\vec{k}_2$. The x and y component of Eq.(4.28) may be written as-[31]

$$D_{n1xx}E_{n1x} + D_{n1xy}E_{n1xy} = -\frac{iJ_{x1}^{NL}}{\omega_1\varepsilon_0}$$
$$-D_{n1xy}E_{n1x} + D_{n1xy}E_{n1xy} = -\frac{iJ_{y1}^{NL}}{\omega_1\varepsilon_0} \quad (4.31)$$

After solving Eq.(4.29), we get

$$E_{n1x} = \frac{2i\omega_1 k_0^2}{c^2\varepsilon_0}\frac{J_{x1}^{NL}}{\left[k_1^2k_{z1}^2 - \frac{\omega_p^4}{c^4}\frac{\omega_1^2}{\omega_c^2}\right]}$$

Here put the value of J_{x1}^{NL}, we get

$$E_{n1x} = \frac{\omega_1 k_0^2}{c^2}\frac{eE_{0x}^*}{m\omega_c}\frac{k^2(1+\chi_{1i})\phi}{\left[k_1^2k_{z1}^2 - \frac{\omega_p^4}{c^4}\frac{\omega_1^2}{\omega_c^2}\right]} \quad (4.32)$$

D_2 may be recovered from replacing ω_1 by ω_2 and $\vec{k}_1$ by $\vec{k}_2$. The x and y component of Eq.(4.30) may be written as [31]-

$$D_{n2xx}E_{n2x} + D_{n2xy}E_{n2xy} = -\frac{iJ_{x2}^{NL}}{\omega_2\varepsilon_0}$$
$$-D_{n2xy}E_{n2x} + D_{n2xy}E_{n2xy} = -\frac{iJ_{y2}^{NL}}{\omega_2\varepsilon_0} \quad (4.33)$$

After solving these equations, we get

$$E_{n2x} = \frac{2i\omega_2 k_0^2}{c^2\varepsilon_0}\frac{J_{x2}^{NL}}{\left[k_2^2k_{z2}^2 - \frac{\omega_p^4}{c^4}\frac{\omega_2^2}{\omega_c^2}\right]}$$

Here put the value of J_{x2}^{NL}, we get[31]-

$$E_{x2} = \frac{\omega_2 k_0^2}{c^2}\frac{eE_{0x}}{m\omega_c}\frac{k^2(1+\chi_{1i})\phi}{\left[k_2^2k_{z2}^2 - \frac{\omega_p^4}{c^4}\frac{\omega_2^2}{\omega_c^2}\right]} \quad (4.34)$$

Substituting for E_{n1x} and E_{n2x} in Eq.(4.26), we obtain the dispersion relation-

$$\varepsilon'\phi = -\chi'_{1e}\,\phi_m$$

Put the value of ϕ_m from Eq.(4.15), we get

$$\varepsilon'\phi = -\chi'_{1e}\frac{e}{m\omega_0\omega_c}\left(E_{0x}E_{n1x} + E^*_{0x}E_{n2x}\right)$$

Put the value of E_{1x} and E_{2x} from Eq.(4.30)&(4.32) ,we get

$$\varepsilon'\phi = -\chi'_{1e}\frac{e}{m\omega_0\omega_c}\left(E_{0x}\frac{\omega_1 k_0^2}{c^2}\frac{eE^*_{0x}}{m\omega_c}\frac{k^2(1+\chi_{1i})\phi}{\left[k_1^2k_{z1}^2 - \frac{\omega_p^4}{c^4}\frac{\omega_1^2}{\omega_c^2}\right]} + E^*_{0x}\frac{\omega_2 k_0^2}{c^2}\frac{eE_{0x}}{m\omega_c}\frac{k^2(1+\chi_{1i})\phi}{\left[k_2^2k_{z2}^2 - \frac{\omega_p^4}{c^4}\frac{\omega_2^2}{\omega_c^2}\right]}\right)$$

$$\varepsilon'\phi = -\chi'_{1e}(1+\chi_{1i})\frac{e}{m\omega_0\omega_c}\left(E_{0x}\frac{\omega_1 k_0^2}{c^2}\frac{eE^*_{0x}}{m\omega_c}\frac{k^2}{\left[k_1^2k_{z1}^2 - \frac{\omega_p^4}{c^4}\frac{\omega_1^2}{\omega_c^2}\right]} + E^*_{0x}\frac{\omega_2 k_0^2}{c^2}\frac{eE_{0x}}{m\omega_c}\frac{k^2}{\left[k_2^2k_{z2}^2 - \frac{\omega_p^4}{c^4}\frac{\omega_2^2}{\omega_c^2}\right]}\right)\phi$$

$$\varepsilon'\phi = -\chi'_{1e}(1+\chi_{1i})\frac{e^2E^*_{0x}E_{0x}}{m^2\omega_0\omega_c^2}\left(\frac{\omega_1 k_0^2}{c^2}\frac{k^2}{\left[k_1^2k_{z1}^2 - \frac{\omega_p^4}{c^4}\frac{\omega_1^2}{\omega_c^2}\right]} + \frac{\omega_2 k_0^2}{c^2}\frac{k^2}{\left[k_2^2k_{z1}^2 - \frac{\omega_p^4}{c^4}\frac{\omega_2^2}{\omega_c^2}\right]}\right)\phi.$$

After rearranging the above equation we get

$$\varepsilon'\phi = -\chi'_{1e}(1+\chi_{1i})\frac{k^2|v_{0x}|^2}{k_0^2c^2}\frac{k_\perp^2/k_0^2}{\frac{k_\perp^4}{k_0^4} - \left[\frac{4k_z}{k_0} - \frac{2\omega}{\omega_0}\right]^2}\phi, \qquad (4.35)$$

where

$$E_{0x}^2 = E_{0x}E^*_{0x},$$

$$|v_{ox}| = \frac{ieE_{0x}}{m\omega_c}\frac{k_{0z}}{k_0}.$$

The dispersion relation is-

$$\varepsilon'\phi = R'\phi \qquad (4.36)$$

where

$$R' = -\chi'_{1e}(1+\chi_{1i})\frac{k^2\left|v_{0x}\right|^2}{k_0^2c^2}\;\frac{k_\perp^2/k_0^2}{\frac{k_\perp^4}{k_0^4}-\left[\frac{4k_z}{k_0}-\frac{2\omega}{\omega_0}\right]^2} \tag{4.37}$$

and

$$\varepsilon' = 1+\chi_e^{'}+\chi_i^{'}+\chi_d \approx \chi_e^{'}+\chi_i^{'}+\chi_d$$

Put the value of $\chi_e^{'}$ and χ'_i in above equation-

$$\chi_e^{'}+\chi_i^{'}+\chi_d = 0$$

$$\frac{\omega_{pi}^2}{k^2c_s^2}\left[1+i\sqrt{\pi}\,\frac{\omega-\omega_m^*}{k_z v_{the}}\right]\left[1+\frac{i\beta}{(\omega+i\eta)}\right]+\frac{\omega_{pi}^2}{k^2c_s^2}\left[\frac{T_e}{T_i}b_{1i}-\frac{\omega_m^*}{\omega}(1-b_{1i})\right]\left[1+\frac{i\beta}{(\omega+i\eta)}\right]+\chi_d = 0$$

$$\left[1+i\sqrt{\pi}\,\frac{\omega-\omega_m^*}{k_z v_{the}}\right]\left[1+\frac{i\beta}{(\omega+i\eta)}\right]+\left[\frac{T_e}{T_i}b_{1i}-\frac{\omega_m^*}{\omega}(1-b_{1i})\right]\left[1+\frac{i\beta}{(\omega+i\eta)}\right]+\frac{k^2c_s^2}{\omega_{pi}^2}\chi_d = 0$$

$$\left[1+i\sqrt{\pi}\,\frac{\omega-\omega_m^*}{k_z v_{the}}\right]\zeta+\left[\frac{T_e}{T_i}b_{1i}-\frac{\omega_m^*}{\omega}(1-b_{1i})\right]\zeta+\frac{k^2c_s^2}{\omega_{pi}^2}\chi_d = 0$$

$$\zeta+i\sqrt{\pi}\,\frac{\omega-\omega_m^*}{k_z v_{the}}\zeta+\frac{T_e}{T_i}b_{1i}\zeta-\frac{\omega_m^*}{\omega}(1-b_{1i})\zeta+\frac{k^2c_s^2}{\omega_{pi}^2}\chi_d = 0$$

$$\zeta+i\sqrt{\pi}\,\frac{\omega-\omega_m^*}{k_z v_{the}}\zeta+\frac{T_e}{T_i}b_{1i}\zeta+\frac{k^2c_s^2}{\omega_{pi}^2}\chi_d = \frac{\omega_m^*}{\omega}(1-b_{1i})\zeta$$

$$\omega = \frac{\omega_m^*(1-b_{1i})\zeta}{\zeta+i\sqrt{\pi}\,\frac{\omega-\omega_m^*}{k_z v_{the}}\zeta+\frac{T_e}{T_i}b_{1i}\zeta+\frac{k^2c_s^2}{\omega_{pi}^2}\chi_d}$$

$$\omega = \frac{\omega_m^*(1-b_{1i})\zeta\left\{\zeta+\frac{T_e}{T_i}b_{1i}\zeta+\frac{k^2c_s^2}{\omega_{pi}^2}\chi_d-i\sqrt{\pi}\,\frac{\omega-\omega_m^*}{k_z v_{the}}\zeta\right\}}{\left(\zeta+\frac{T_e}{T_i}b_{1i}\zeta+\frac{k^2c_s^2}{\omega_{pi}^2}\chi_d\right)^2-\left(i\sqrt{\pi}\,\frac{\omega-\omega_m^*}{k_z v_{the}}\zeta\right)^2}$$

$$\omega = \frac{\omega_m^* (1-b_{1i})\zeta \left(\zeta + \frac{T_e}{T_i} b_{1i}\zeta + \frac{k^2 c_s^2}{\omega_{pi}^2}\chi_d \right)}{\left(\zeta + \frac{T_e}{T_i} b_{1i}\zeta + \frac{k^2 c_s^2}{\omega_{pi}^2}\chi_d \right)^2} \left(1 - i\sqrt{\pi} \frac{\omega - \omega_m^*}{k_z v_{th} \left(\zeta + \frac{T_e}{T_i} b_{1i}\zeta + \frac{k^2 c_s^2}{\omega_{pi}^2}\chi_d \right)} \zeta \right)$$

In the absence of the pump excluded Eq. (4.33)-

$$\omega = \frac{\omega_m^* (1-b_{1i})\zeta}{\left(\zeta + \frac{T_e}{T_i} b_{1i}\zeta + \frac{k^2 c_s^2}{\omega_{pi}^2}\chi_d \right)} \left(1 - i\sqrt{\pi} \frac{\omega - \omega_m^*}{k_z v_{the} \left(\zeta + \frac{T_e}{T_i} b_{1i}\zeta + \frac{k^2 c_s^2}{\omega_{pi}^2}\chi_d \right)} \zeta \right) \quad (4.38)$$

Instability occurs when $\omega < \omega^*$ with the pump included in eq. (33) ,we get

$$\omega = \frac{\omega_m^* (1-b_{1i})\zeta}{\left(\zeta + \frac{T_e}{T_i} b_{1i}\zeta + \frac{k^2 c_s^2}{\omega_{pi}^2}\chi_d - R' \frac{k^2 c_s^2}{\omega_{pi}^2} \right)} \left(1 - i\sqrt{\pi} \frac{\omega - \omega_m^*}{k_z v_{th} \left(\zeta + \frac{T_e}{T_i} b_{1i}\zeta + \frac{k^2 c_s^2}{\omega_{pi}^2}\chi_d - R' \frac{k^2 c_s^2}{\omega_{pi}^2} \right)} \zeta \right) \quad (4.39)$$

For the growth rate writing $\omega = \omega_r + i\gamma$,and considering imaginary part of Eq.(4.39),we get

$$\omega_r + i\gamma = \frac{\omega_m^* (1-b_{1i})\zeta}{\left(\zeta + \frac{T_e}{T_i} b_{1i}\zeta + \frac{k^2 c_s^2}{\omega_{pi}^2}\chi_d - R \frac{k^2 c_s^2}{\omega_{pi}^2} \right)} - i\sqrt{\pi} \frac{\omega_m^* (1-b_{1i})\zeta^2 (\omega - \omega^*)}{k_z v_{the} \left(\zeta + \frac{T_e}{T_i} b_{1i}\zeta + \frac{k^2 c_s^2}{\omega_{pi}^2}\chi_d - R \frac{k^2 c_s^2}{\omega_{pi}^2} \right)^2}$$

$$\gamma = \sqrt{\pi} \frac{\omega_m^* (1-b_{1i})\zeta^2 (\omega - \omega_m^*)}{k_z v_{the} \left(\zeta + \frac{T_e}{T_i} b_{1i}\zeta + \frac{k^2 c_s^2}{\omega_{pi}^2}\chi_d - R \frac{k^2 c_s^2}{\omega_{pi}^2} \right)^2} \quad (4.40)$$

where

$$\zeta = \left(1 + \frac{i\beta}{(\omega + i\eta)} \right)$$

$\beta = \frac{n_{oD} |I_{0e}|}{e n_{oe}}$ is coupling parameter

$$\eta = 0.79a\left(\frac{\omega_{pi}}{\lambda_{Di}}\right)\left(\frac{1}{\delta}\right)\left(\frac{m_i T_i}{m_e T_e}\right) \approx 10^{-2}\omega_{pe}\left(\frac{a}{\lambda_{De}}\right)\left(\frac{1}{\delta}\right)$$

$$\mathrm{bi} = \frac{\mathrm{k}_\perp^2 \mathrm{v}_{\mathrm{thi}}^2}{2\omega_{\mathrm{ci}}}$$

$$\omega^* = \frac{\mathrm{k}_\perp^2 \mathrm{v}_{\mathrm{thi}}^2}{\omega_{\mathrm{c}} \mathrm{L}_{\mathrm{n}}} = \left(\frac{2\mathrm{bi}}{\mathrm{kL}_{\mathrm{n}}}\right)\left(\frac{\mathrm{T}_{\mathrm{e}}}{\mathrm{T}_{\mathrm{i}}}\right)\omega_{\mathrm{ci}}$$

$$\mathrm{R} = \left\{\frac{\omega_{\mathrm{pi}}^2}{\mathrm{k}^2 \mathrm{c}_{\mathrm{s}}^2} + \frac{\mathrm{T}_{\mathrm{e}}}{\mathrm{T}_{\mathrm{i}}}\mathrm{b}_{\mathrm{i}}\left(\frac{\omega_{\mathrm{pi}}^2}{\mathrm{k}^2 \mathrm{c}_{\mathrm{s}}^2}\right)^2 - \frac{\omega^*}{\omega}\left(1-\mathrm{b}_{\mathrm{i}}\right)\left(\frac{\omega_{\mathrm{pi}}^2}{\mathrm{k}^2 \mathrm{c}_{\mathrm{s}}^2}\right)^2\right\}\frac{\mathrm{k}^2\left|\mathrm{v}_{0\mathrm{x}}\right|^2}{\mathrm{k}_0^2 \mathrm{c}^2}\,\frac{\mathrm{k}_\perp^2/\mathrm{k}_0^2}{\frac{\mathrm{k}_\perp^4}{\mathrm{k}_0^4} - \left[\frac{4\mathrm{k}_{\mathrm{z}}}{\mathrm{k}_0} - \frac{2\omega}{\omega_0}\right]^2}$$

$$-\mathrm{i}\left\{\sqrt{\pi}\,\frac{\omega_{\mathrm{pi}}^2}{\mathrm{k}^2 \mathrm{c}_{\mathrm{s}}^2}\,\frac{\omega-\omega^*}{\mathrm{k}_{\mathrm{z}} \mathrm{v}_{\mathrm{th}}}\,\frac{\omega^*}{\omega}\left(1-\mathrm{b}_{\mathrm{i}}\right)\left(\frac{\omega_{\mathrm{pi}}^2}{\mathrm{k}^2 \mathrm{c}_{\mathrm{s}}^2}\right) - \frac{\mathrm{T}_{\mathrm{e}}}{\mathrm{T}_{\mathrm{i}}}\mathrm{b}_{\mathrm{i}}\left(\frac{\omega_{\mathrm{pi}}^2}{\mathrm{k}^2 \mathrm{c}_{\mathrm{s}}^2}\right) - 1\right\}\frac{\mathrm{k}^2\left|\mathrm{v}_{0\mathrm{x}}\right|^2}{\mathrm{k}_0^2 \mathrm{c}^2}\,\frac{\mathrm{k}_\perp^2/\mathrm{k}_0^2}{\frac{\mathrm{k}_\perp^4}{\mathrm{k}_0^4} - \left[\frac{4\mathrm{k}_{\mathrm{z}}}{\mathrm{k}_0} - \frac{2\omega}{\omega_0}\right]^2}$$

CHAPTER 5

RESULTS AND CONCLUSION

5.1 RESULTS AND CONCLUSION

For my present calculation, I have used typical dusty plasma parameters which are-

Temperature of ion, T_i =1KeV Temperature of electron, Te =1.5 KeV Thermal velocity of ion. $v_{thi} = 10^5 \, m/sec$ Thermal velocity of electron $v_{the}=2\times10^6$ m/sec guide magnetic field B_0=2.4KG Electric field E_0=0.50 V/cm Electron collision frequency, $\nu_e=4\times10^5$/sec Ion sound speed $C_S=8\times10^4$ cm/sec Electron plasma density, $n_{0e}=10^{10} - 2 \times 10^9 cm^{-3}$ Ion plasma density $n_{0i}=10^8$ cm^{-3} Magnetic field=2×10^4T Dust density $n_{0D}=4\times10^4$-8×10^5 cm^{-3} Dust grain size, $a = 10^{-4} - 4 \times 10^{-4}$ cm Ratio of $\frac{\omega_0}{\omega_{ci}} = 60$ Mass of electron, $m_{0e} = 9.1 \times 10^{-28}$ g Mass of ion, $m_{0i} = 40 \times 1836 m_{0e}$ (Potassium plasma) Charge on electron, e = 4.8 x10 $^{-10}$esu Speed of light, c = 3 x 10^{10} cm/s $k_0 Ln = 10$	Normal Frequency $\omega = 10^{10}$ rad / sec Frequency $\beta=8\times10^5$/sec $\frac{\lvert v_{0x}\rvert^2}{v_{thi}^2}$ =9 when pump present $\frac{\lvert v_{0x}\rvert^2}{v_{thi}^2}$ =0 when no pump $\frac{\omega_{ci}}{k_z v_{th}}$ =10, 6.67, 5 $m/m_i=1.3\times10^{-5}$ [potassium]

The above mentioned parameter have been used the present calculation.
The graphs have been plotted using origin pro software.

5.1.1 Graph between growth rate γ vs δ(=n_{oi}/n_{oe})

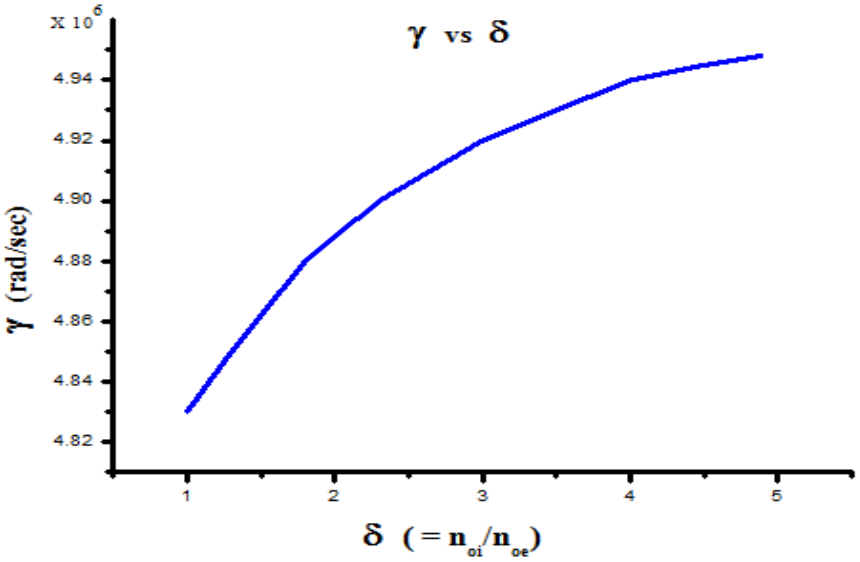

In this graph we can see that the growth rate increases with relative density of dust grain size (δ).

5.1.2 Graph between growth γ vs a (cm)

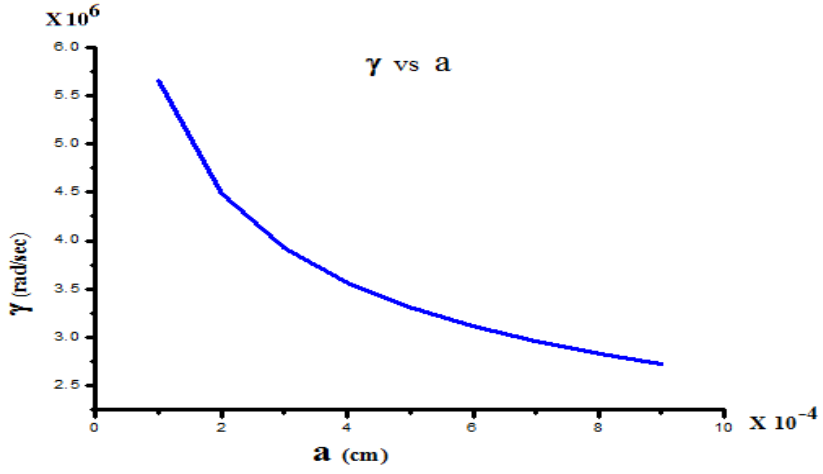

From the graph we can say that the growth decreases with dust grain size (a).

5.1.3 Graph between growth γ vs n_{0d} (cm^{-3})

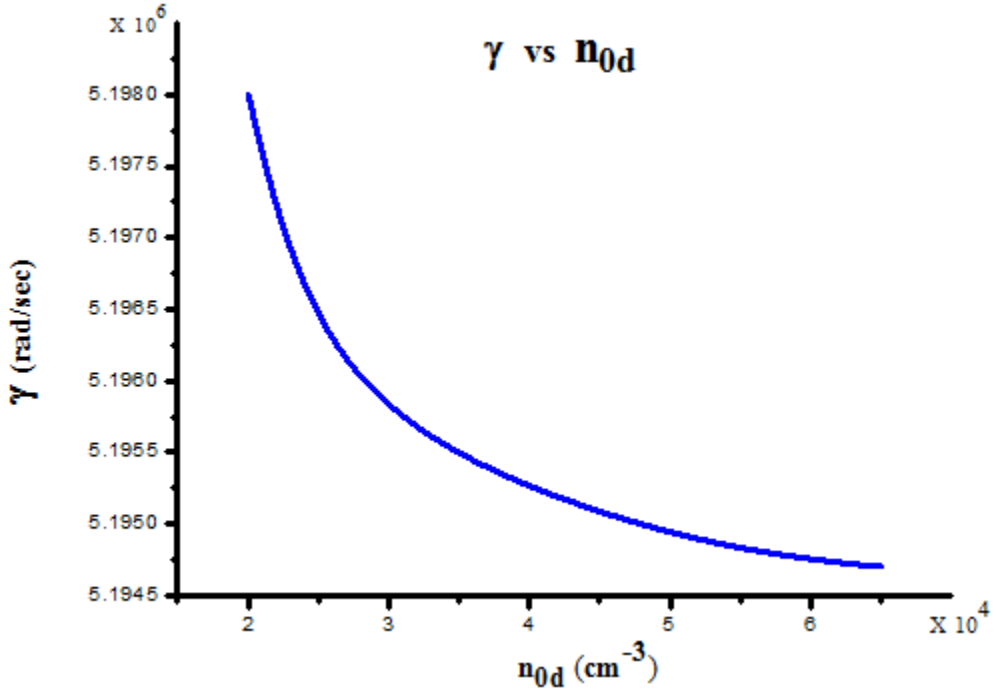

The graph shows that the growth rate decreases with dust grain density.

Conclusion-

We have examined the role of dust grains on fast wave stabilization/destabilization of drift wave in plasma. We have found that

(1) The growth rate (γ) of the mode increases with the relative density of dust grain (δ).

(2) The value of growth (γ) decreases with the dust grain size (a).

(3) The value of growth (γ) decreases with dust grain density (n_{0d}).

6: References

[1] Bellan ,P.M. *Fundamentals of Plasma Physics*,(Cambridge University Press, Cambridge, 2006).

[2] Callen J.D. *Fundamentals of Plasma Physics* (University of Wisconsin,Madison,2006).

[3] Opher M. . Silva L. O Dauger D. E. Decyk V.K. and. Dawson J. M Phys. Plasmas 8, 2454 (2001).

[4] Bittencourt J.A, Fundamentals of Plasma Physics / Ch. 1 / Page 2(Springer 2004)

[5] Shukla P. K. and Mamun. A. A., Introduction to Dusty Plasma Physics. Institute of Physics Publishing Ltd., 2002.

[6] Goldston Robert J. and Rutherford Paul H. , Introduction to plasma physics / Institute of Physics Publishing Bristol and Philadelphia Ltd.,1995

[7] Chen F. F., Introduction to plasma physics and controlled fusion . Volume 1, Plasma physics, (Springer, 2006)

[8] W. Horton, Rev. Mod. Phys. 71, 735 (1999).

[9] H. W. Hendel, T. K. Chu, and P. A. Politzer, Phys. Fluids 11, 2426 (1968).

[10] W. M. Hooke and S. Bernabei, Phys. Rev. Lett. 28, 407 (1972).

[11] Y. S. Satya and P. K. Kaw, Phys. Rev. Lett. 31, 1453 (1973).

[12] W. Horton ,Drift Waves and Transport, Institute for Fusion Studies, The University of Texas, Austin, Texas 78712

[13] C. S. Liu, M. N. Rosenbluth, and C. W. Horton, Jr., Phys. Rev. Lett. 29, 1489 (1972).

[14] W. Horton, Phys. Rev. Lett. 37, 1269 (1976).

[15] D. W. Ross and S. M. Mahajan, Phys. Rev. Lett. 40, 324 (1978).

[16] J. D. Callen, Phys. Rev. Lett. 39, 1540 (1977).

[17] Y. C. Lee and L. Chen, Phys. Rev. Lett. 42, 708 (1979)
.
[18] A. Hasegawa, Phys. Rev. Lett. 27, 11 (1971).

[19] Y. Nishida, M. Tanibayashi, and K. Ishii, Phys. Rev. Lett. 24, 1001 (1970).

[20] M. W. Alcock and B. E. Keen, Phys. Rev. Lett. 26, 1426 (1971).

[21] S. Sen and R. A. Cairns, Phys. Plasmas 5, 4280 (1998).

[22] R. Gore, J. Grun, and H. Lashinsky, Phys. Rev. Lett. 40(17), 1140 (1978)
.
[23] C. S. Liu and V. K. Tripathi, Phys. Fluids 23, 345 (1980).

[24] A. Kuley and V. K. Tripathi, Phys. Plasmas 16, 032504 (2009).

[25] A. M. DuBois, A. C. Eadon, and E. Thomas, Jr., Phys. Plasmas 19, 072102 (2012).

[26] P. K. Kaw, Advances in Plasma Physics, edited by A. Simon and W. B. Thompson (Wiley, New York, 1976), Vol. 6, p. 179.

[27] C. S. Liu and V. K. Tripathi, Phys. Rep. 130(3), 143 (1986).

[28] Suresh C. Sharma and Jyotsna Sharma Phys. Plasmas **17**, 043704 (2010)

[29] Ved Prakash,Vijayshri,Suresh C. Sharma,and Ruby Gupta Phys. Plasmas 20, 053701 (2013)

[30] Animesh Kuley, C. S. Liu,and V. K. Tripathi Phys. Plasmas **17**, 072506 (2010)

[31] Pawan Kumar and V. K. Tripathi Phys. Plasmas 20, 032502 (2013)

[32] Ashok Kumar and V. K. Tripathi Phys. Plasmas **15**, 062509 (2008)

[33] T. Ohkawa, Kaku Yugo Kenkyu, Bessatsu **37**, 117,1977
.
[34] 4. J. Winter and G. Gebauer, J. Nucl. Mater. **266-269**, 228,1999.

[35] M.F..Bashir , *Drift Effects on Plasma Waves* (COMSATS Institute of Information Technology , 2014).

[36] https://www.euro-fusion.org/2011/09/tokamak-principle-2/

[37] Barkan, A., D'Angelo, N. and Merlino, R. L., Experiments on ion-acoustic waves in dusty plasmas.*Planet. Space Sci.* Vol. 44. No 3. pp. 239-242,1996.

[38] Chu J H and I L 1994 *Phys. Rev. Lett.* **72,**4009.

[39] http://web.ics.purdue.edu/~nowack/geos105/lect18-dir/lecture18.htm

[40] http://www.laetusinpraesens.org/iter/iter8.php

[41] Fortov V.E., Nefedov A. P., Torchinsky V.M., Molotkov V I, Petrov O.F, Samarian A .A, Lipaev A. M. and Khrapak A. G. 1997 *Phys. Lett.* A **229,**317.

[42] Jana M. R., Sen A, and Kaw P. K., Phys. Rev. E 48, 3930 (1993).